EE 541, FALL 2006: COURSE NOTES #2

# Scattering Parameters: Concept, Theory, and Applications

**Dr. John Choma**
Professor of Electrical & Systems Architecture Engineering

**University of Southern California**
**Department of Electrical Engineering-Electrophysics**
**University Park: Mail Code: 0271**
**Los Angeles, California 90089–0271**

**213–740–4692 [USC Office]**
**213–740–8677 [USC Fax]**
**johnc@usc.edu**

## *ABSTRACT:*

*This report introduces the scattering parameter concept from two perspectives. First, the scattering parameters are shown to be an effective vehicle for characterizing the high frequency I/O characteristics of two port networks. Such measurement effectiveness derives from the fact that scattering parameter measurements obviate problems invariably incurred at very high frequencies by the actions of either short-circuiting or open circuiting network ports. The second perspective is the utility of scattering analyses in the design of lossless two port filters, which are fundamental to modern communication systems.*

**Original: November 2002**

# 1.0. INTRODUCTION

The short circuit admittance, open circuit impedance, hybrid h–, and hybrid g–parameters are commonly used to formulate two port circuit models that macroscopically interrelate the driving point input and output impedance and forward and reverse transfer characteristics of relatively complex linear networks. These models are simple architectures in that they embody only four electrical parameters whose measurement or calculation exploit the electrical implications of short or open circuits imposed at the input and output ports of the network undergoing study. Although the parameterization of these conventional two port models can generally be executed straightforwardly and accurately at relatively low signal frequencies, high signal processing frequencies present at least two challenges in broadband electronics. The first of these challenges is that the unavoidable parasitic inductance implicit to circuit interconnects renders perfect short circuits an impossibility at very high signal frequencies. Moreover, very low impedance paths at either the input or the output port of electronic circuits may force embedded active devices to function nonlinearly or even to fail because of excessive current conduction. Second, the inherent potential instability of most high frequency or broadband electronic networks is exacerbated when these networks are constrained to operate with open circuited input or output ports. For example, attempts to measure the open circuit impedance parameters of a broadband electronic circuit are invariably thwarted by parasitic network oscillations incurred by the action of opening either an input or an output network port.

The daunting, if not impossible, challenge posed by the measurement of conventional two port parameters motivates the scattering, or S–parameter characterization of linear two port systems. In contrast to the impedance, admittance, and hybrid parameters, the scattering parameters of linear electrical or electronic networks are measured without need of short-circuiting or open circuiting input and output ports. Instead, these ports are terminated in fixed and known characteristic impedances that are often similar or even identical to the terminating impedances incorporated in the design. Accordingly, the dynamic performance and operational integrity of a network under test are not compromised by test fixturing adopted for its scattering parameter characterization. Neither is the comfort level most engineers have with conventional two port parameters compromised, for measured scattering parameters can always be converted to corresponding admittance, impedance, and hybrid parameters. While such conversion practices are ubiquitous, they are actually unnecessary since the driving point and transfer properties of linear passive or active two port configurations can be determined directly in terms of the measured or computed network S–parameters.

The preceding paragraph implies that S–parameters are a measurement-friendly alternative to conventional two port network parameters. Indeed, scattering parameters are conveniently extracted in the laboratory, but they are also explicitly useful in design. Because the S–parameters of a linear two port network interrelate incident and reflected waves of energy at input and output ports, as opposed to intertwining input and output port voltages and currents, they are useful in the design of microwave amplifiers. The reason underlying this design utility is that voltages and currents are more difficult to quantify uniquely at microwave frequencies than are delivered energies and average signal power levels. Additionally, the scattering parameters of lossless two ports have a unique property that enables their judicious exploitation in the design of lossless matching networks serving to achieve maximum signal power transfer from a source to its load.

This report develops the scattering parameter concept and defines the S–parameters of a generalized linear two port network. Following a demonstration of the strategy used to convert S–parameters to conventional two port parameters, it addresses the utility of S–parameters in the analysis of active networks. Finally, the report explores the application of S–parameters in the design of lossless matching filters for RF circuit applications.

# 2.0. REFLECTION COEFFICIENT

The scattering parameter concept for two port network analyses is best introduced by first considering the scattering characterization of the simple one port network consisting of the load impedance, $Z_l$, shown in Figure (1). The load impedance at hand consists of a real part, say $R_l$, and an imaginary component, $X_l$, which is positive for an inductive termination and negative for a capacitive load. The subject figure portrays a voltage source, $V_s$, whose Thévenin equivalent impedance is the real resistance, $R_o$. In the scattering theory vernacular, this Thévenin impedance is often referred to as the reference impedance of the one port network.

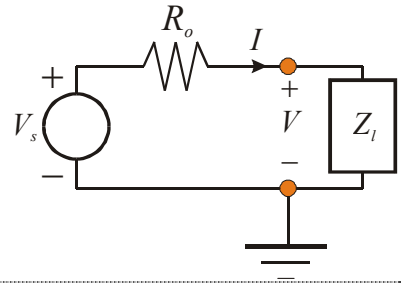


**Fig. (1).** A One Port Load Impedance Driven By A Voltage Source Whose Thévenin Equivalent Resistance Is $R_o$.

Let the current, $I$, conducted by the load be decomposed into the algebraic superposition of an incident current, $I_i$, and a reflected, or "scattered" current, $I_r$, such that

$$I = I_i - I_r \ . \tag{1}$$

In the last relationship, $I_i$ is defined as the value of current $I$ for the special case of a load impedance, $Z_l$, matched to the one port reference impedance, $R_o$; that is, $Z_l \equiv R_o$. Thus,

$$I_i = \frac{V_s}{2R_o}, \tag{2}$$

whence the reflected current, $I_r$, follows as

$$I_r = I_i - I = \frac{V_s}{2R_o} - \frac{V_s}{R_o + Z_l} = \left(\frac{Z_l - R_o}{Z_l + R_o}\right)\frac{V_s}{2R_o} \ . \tag{3}$$

The parenthesized quantity on the far right hand side of (3) is known as the scattering parameter, or more simply, the reflection coefficient, $\rho$, of the considered one port network. Specifically,

$$\rho \triangleq \frac{Z_l - R_o}{Z_l + R_o} = \frac{Z_{ln} - 1}{Z_{ln} + 1}, \tag{4}$$

where

$$Z_{ln} = Z_l / R_o \tag{5}$$

is the load impedance normalized to the system reference impedance. Note that (4) and (2) allow (3) to be expressed as

$$I_r = \rho I_i , \tag{6}$$

which implies that the net load current in (1) can be written as

$$I = (1 - \rho) I_i . \tag{7}$$

Equation (7) confirms that the only current supplied by the signal source is the incident current when $\rho = 0$, which corresponds to a terminating load impedance matched to the reference impedance.

## 2.1. VOLTAGE SCATTERING

The load voltage, $V$, can be similarly decomposed into an incident component, $V_i$, and a reflected component, $V_r$, in accordance with

$$V = V_i + V_r . \tag{8}$$

The incident load voltage is the value of voltage $V$ under the condition of a load impedance matched to the circuit reference impedance; that is,

$$V_i = \left( \frac{Z_l}{R_o + Z_l} \right) V_s \Big|_{Z_l = R_o} = \frac{V_s}{2} . \tag{9}$$

It follows that the scattered load voltage component is

$$V_r = \left( \frac{Z_l - R_o}{Z_l + R_o} \right) \frac{V_s}{2} = \rho V_i , \tag{10}$$

which allows the net load voltage to be expressed as

$$V = (1 + \rho) V_i . \tag{11}$$

Observe from (6), (9), and (10) that

$$V_i = R_o I_i , \tag{12}$$

and

$$V_r = R_o I_r . \tag{13}$$

## 2.2. POWER SCATTERING

The signal power, $P$, delivered to the load impedance can also be written as a superposition of incident $(P_i)$ and scattered $(P_r)$ powers; that is,

$$P = P_i - P_r \ . \tag{14}$$

If the load voltage, $V$, is a sinusoid of amplitude $V_p$, the average incident power delivered to the matched load is

$$P_i = \frac{\left(V_p/\sqrt{2}\right)^2}{R_o} = \frac{V_s^2}{8R_o}, \tag{15}$$

where $V_s$ symbolizes the amplitude of the applied sinusoidal input voltage. The average power dissipated in the actual load impedance is

$$P = \frac{|I|^2 R_l}{2} = \frac{V_s^2 R_l}{2|Z_l + R_o|^2}. \tag{16}$$

A bit of algebra applied to the combination of (14), (15), and (16) confirms that

$$P_r = |\rho|^2 P_i \ , \tag{17}$$

whereupon the average dissipated load power is seen as

$$P = \left(1 - |\rho|^2\right) P_i = \left(1 + |\rho|\right)\left(1 - |\rho|\right) P_i \ . \tag{18}$$

Thus, if the load impedance were to be matched to the circuit reference impedance, $\rho$ is zero, and no power is scattered back to the signal source from the load.

## 2.3. SIGNIFICANCE OF THE REFLECTION COEFFICIENT

The reflection coefficient introduced in (4) is a bilinear transformation that encodes ohms in the Cartesian impedance plane to a dimensionless complex number in the reflection plane. Because of the bilinear nature of this transformation, the reflection coefficient of an impedance is unique for a given impedance function and conversely, a unique impedance derives from a stipulated reflection coefficient. To demonstrate the latter contention, (4) can be solved for load impedance $Z_l$ to obtain

$$Z_l = \left(\frac{1+\rho}{1-\rho}\right) R_o \ , \tag{19}$$

which certainly assures uniqueness of impedance for any given value of reflection coefficient. The engineering implication of this uniqueness is that the measurement of the reflection coefficient for a one port network, as is routinely accomplished by laboratory network analyzers, is equivalent to a determination of the impedance that terminates the characterized one port.

Assuming that the real part of the load impedance is non-negative for all signal frequencies, which is tantamount to asserting that $Z_l$ is a passive two terminal impedance, (4) shows that the magnitude of the load reflection coefficient is at most unity. Note that for a short-circuited load impedance *($Z_l = 0$)*, $\rho = -1$, while an open-circuited load *($Z_l = \infty$)* produces $\rho = 1$. In view of the fact that the magnitude of $\rho$ can never exceed unity for passive loads, it follows that all possible passive impedances whose values reflect a range extending from a short circuit to an open circuit map to coordinates lying within, or directly on, the unit circle centered at the origin of the reflection plane. This observation is dramatized in Figure (2), where the reflection plane is

taken as a coordinate system whose horizontal axis is the real part of $\rho$ and whose vertical axis is the imaginary part of $\rho$. If, for example, $\rho_r = 0.3$ and $\rho_i = 0.75$ in the subject figure, the normalized impedance is, from (19), $Z_l/R_o = 0.3302 + j1.425$. If the reference impedance is *50 ohms* and the signal frequency is *1 GHz*, this normalized impedance consists of the series combination of a resistance of *16.51 ohms* and an inductance of *11.34 nanohenries*.

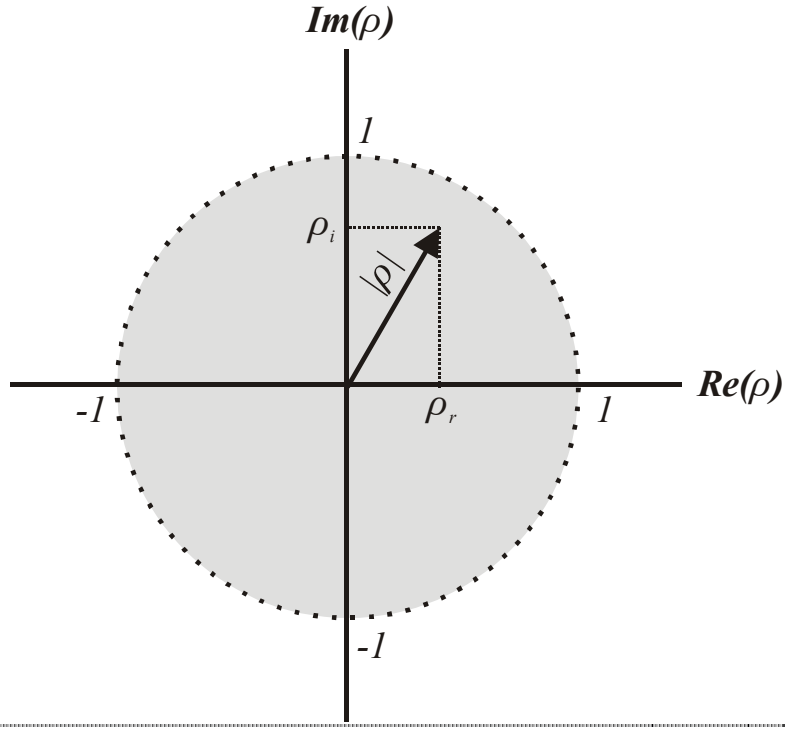


**Fig. (2).** Cartesian Coordinate System Of The Reflection Coefficient Plane. The Shaded Area Enclosed By The Unit Circle Centered At The Origin Of The Plane Is The Loci Of All Possible Passive Load Impedances. The Indicated Vector Symbolizes A Reflection Coefficient, $\rho$, of $\rho_r + j\rho_i$, Which Corresponds To The Unique One Port Impedance Function, $Z_l$, Defined By Equation (19).

The disclosure of a unit circle boundary for the reflection coefficient magnitude is worthy of elaboration. To this end, let the reflection coefficient, $\rho$, in (19) be written as $\rho = \rho_r + j\rho_i$, whence the normalized load impedance, $Z_{ln}$, becomes

$$Z_{ln} = \frac{(1+\rho_r)+j\rho_i}{(1-\rho_r)-j\rho_i} = \frac{\left[1-\left(\rho_r^2+\rho_i^2\right)\right]+j(2\rho_i)}{(1-\rho_r)^2+\rho_i^2}. \tag{20}$$

If the normalized impedance is viewed as a series interconnection of a normalized resistance, $R_{ln}$, and a normalized reactance, $X_{ln}$, (20) shows that

$$R_{ln} = \frac{1-\left(\rho_r^2+\rho_i^2\right)}{(1-\rho_r)^2+\rho_i^2} \tag{21}$$

and

$$X_{ln} = \frac{2\rho_i}{\left(1-\rho_r\right)^2 + \rho_i^2} \,. \tag{22}$$

Equations (21) and (22) illuminate several reflection plane properties that comprise the foundation of the Smith chart[1]-[2], a graphical tool used in the analysis of distributed transmission lines and in the design of many linear communication and microwave circuits. The first of these important properties derives from the observation that the relationship, $\rho_r^2 + \rho_i^2 = 1$, defines the unit circuit centered at the origin, $(\rho_r, \rho_i) = (0, 0)$, of the reflection coefficient plane. Accordingly, (21) implies that the area bounded by this unit circle corresponds to positive real part load impedances $(R_{ln} > 0)$, as is suggested in Figure (2). On the other hand, the area outside of the unit circle defined by $\rho_r^2 + \rho_i^2 > 1$, is seen as embracing load impedances having the negative real parts that can be generated by active, potentially unstable, structures. Equation (21) further confirms that all points lying precisely on the subject unit circle itself are in one to one correspondence with purely imaginary one port impedances; that is, $R_{ln} = 0$.

A second set of properties is highlighted by (22). Specifically, purely real load impedances $(X_{ln} = 0)$ imply $\rho_i = 0$. For a passive one port, $\rho_i = 0$ corresponds to all points lying within the unit circle and directly on the horizontal axis of the reflection plane. On the other hand, inductive loads $(X_{ln} > 0)$ in passive one port networks map into the region of the unit circle lying above the horizontal axis, while capacitive passive loads $(X_{ln} < 0)$ establish loci within the unit circle and below the horizontal axis of the reflection plane. These observations, as well as those of the preceding paragraph are summarized in Figure (3).

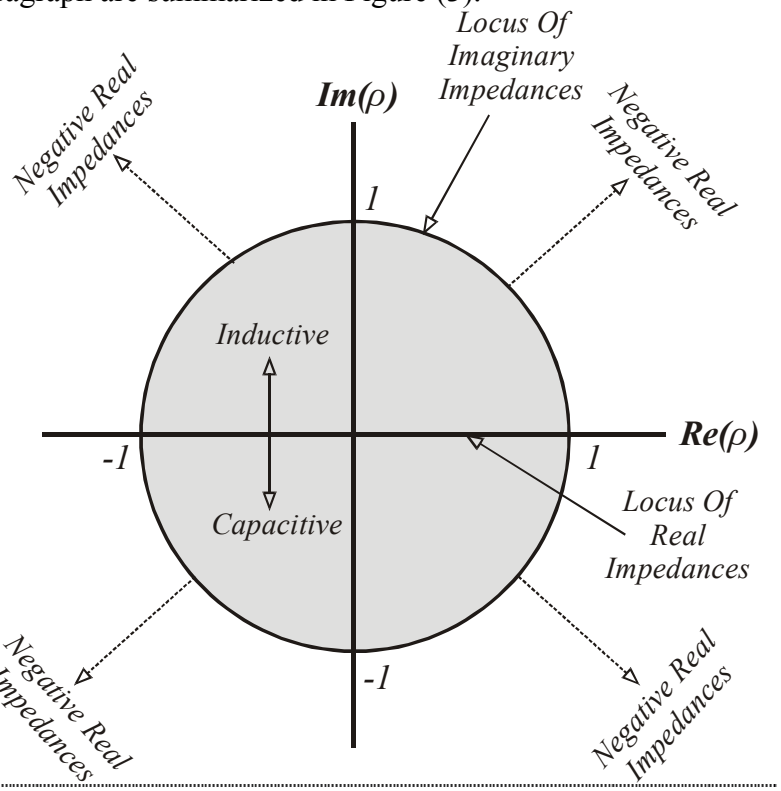


**Fig. (3).** The Impedance Implications Of Reflection Coefficient Loci. The Shaded Region Bounded By The Unit Circle Corresponds To All Impedances Characterized By Positive Real Part Components.

A generalization of the foregoing insights follows from recasting (21) in the form

$$\left(\rho_r - \frac{R_{ln}}{R_{ln}+1}\right)^2 + \rho_i^2 = \left(\frac{1}{R_{ln}+1}\right)^2 . \tag{23}$$

This relationship stipulates that the reflection plane loci of constant real part load impedance are circles centered on the horizontal axis at $\rho_r = R_{ln}/(R_{ln}+1)$ and having radii of $1/(R_{ln}+1)$. To this end, infinitely large real part load impedance is seen to be a point located at $(\rho_r, \rho_i) = (1, 0)$. In concert with a previous discourse, observe in (23) that zero real part load impedance corresponds to the infinity of points lying on the unit circle centered at the origin of the reflection coefficient plane. Figure (4) provides a graphical overview of these observations.

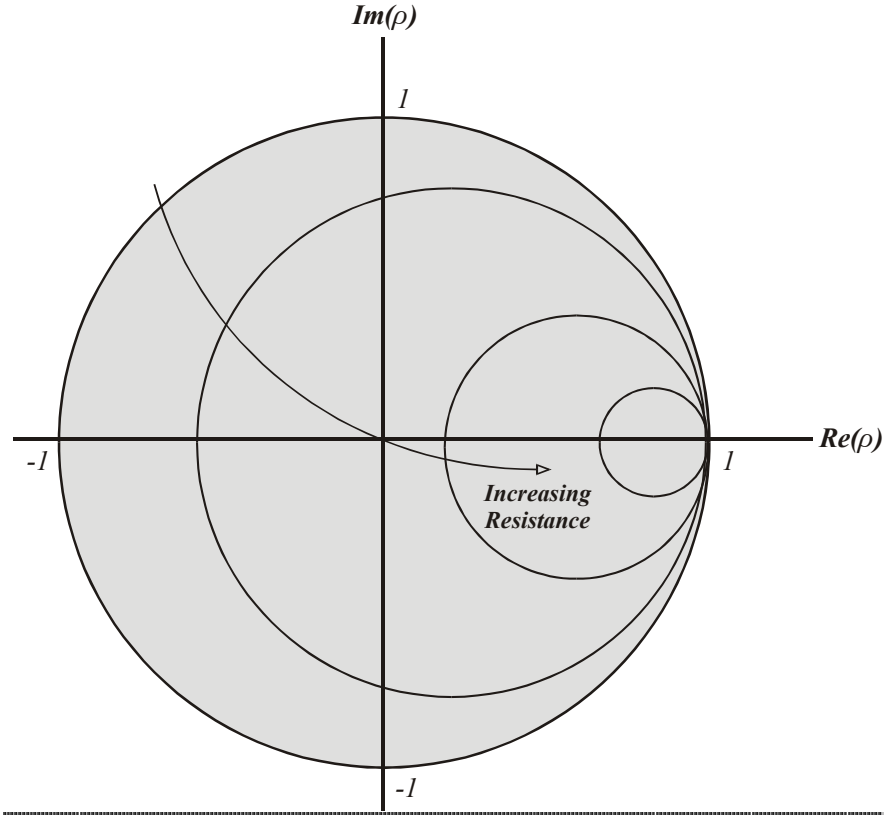


**Fig. (4).** The Contours of Constant Real Part Load Impedance In The Reflection Coefficient Plane.

It is also interesting to learn that constant load reactances also map to circles in the $\rho$-plane. In particular, (22) can be shown to be equivalent to

$$(\rho_r - 1)^2 + \left(\rho_i - \frac{1}{X_{ln}}\right)^2 = \left(\frac{1}{X_{ln}}\right)^2 . \tag{24}$$

The subject constant reactance circles are centered at $(\rho_r, \rho_i) = (1, 1/X_{ln})$ and have radii of $1/X_{ln}$. Note therefore that the centers of these circles are located above the horizontal reflection plane axis for inductive loads and below the horizontal axis for capacitive loads.

The reflection coefficient in (4) can be partitioned into its explicit real and imaginary parts to allow for the plotting of the reflection coefficient contour into a Smith-type chart. To this end, write the normalized load impedance, $Z_{ln}$, in the form, $Z_{ln} = R_{ln} + jX_{ln}$, to obtain $\rho = \rho_r + j\rho_i$, where

$$\rho_r = \frac{R_{ln}^2 - 1}{(R_{ln}+1)^2 + X_{ln}^2} \tag{25}$$

and

$$\rho_i = \frac{2X_{ln}}{(R_{ln}+1)^2 + X_{ln}^2} . \tag{26}$$

As signal frequency is varied, $R_{ln}$ and $X_{ln}$ can be computed, whence the real and imaginary parts of the reflection coefficient in (25) and (26), respectively, can be evaluated for each frequency of interest. The resultant plot of $\rho_i$ -versus- $\rho_r$ comprises the resultant reflection contour, with signal frequency used as an implicit parametric variable.

Equation (26) suggests that the imaginary part of the reflection coefficient is a non-monotonic function of the normalized reactive component of the port impedance undergoing characterization. Specifically, observe that $\rho_i$ is zero at both $X_{ln} = 0$ and $X_{ln} = \infty$, which implies that $\rho_i$ is maximized at an intermediate value of $X_{ln}$, say $X_{lno}$, that constrains the slope, $d\rho_i/dX_{ln}$, to zero. It is a simple matter to show that

$$X_{lno} = \pm(R_{ln}+1) , \tag{27}$$

for which the corresponding reflection coefficient, say $\rho_o$, is

$$\rho_o = \left(\frac{1}{R_{ln}+1}\right)\left(\frac{R_{ln}-1}{2} \pm j\right) . \tag{28}$$

It is understood that the positive algebraic sign in (27) and (28) applies for inductive port impedances, while the negative sign pertains to capacitive loads. As is demonstrated in the following example, (27) boasts at least tacit engineering significance when it is applied to lowpass dominant pole networks. For such networks, the frequency implied by (27) is the *3-dB* bandwidth of the network formed by driving the subject impedance with a voltage source whose Thévenin resistance is the reference resistance used in the impedance characterization.

## EXAMPLE #1:

Plot the real and imaginary parts of the reflection coefficient, as a function of signal frequency, for the impedance established by the lowpass RC network in Figure (5a). The indicated series circuit resistance, $R$, is *300 Ω*, while the capacitance, $C$, is *50 pF*. The normalizing reference impedance *($R_o$)* can be taken to be *50 Ω*.

## SOLUTION:

**(1).** The impedance of the RC network in Figure (5a) is

$$Z_1 = R + \frac{1}{j\omega C} ,$$

whence the normalized load resistance is

$$R_{ln} = \frac{R}{R_o}$$

and the normalized load reactance is

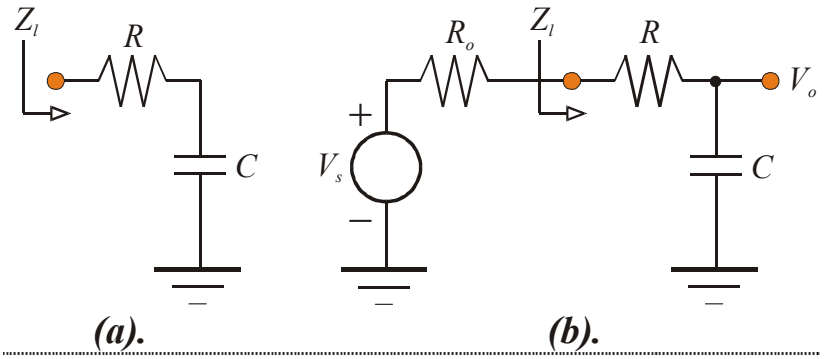


**Fig. (5).** **(a).** Series RC Lowpass Filter Addressed In Example #1. **(b).** The Filter In (a) Driven By A Voltage Source Having A Thévenin Internal Resistance Of $R_o$, The Reference Impedance Used In The Characterization Of The RC Load Impedance.

$$X_{ln} = -\frac{1}{\omega R_o C} .$$

**(2).** The foregoing expressions for $R_{ln}$ and $X_{ln}$ can be substituted into (25) and (26) to deduce the frequency dependencies of the real and imaginary parts of the reflection coefficient in the stipulated *50 Ω* reference environment. The pertinent plots are displayed in Figure (6).

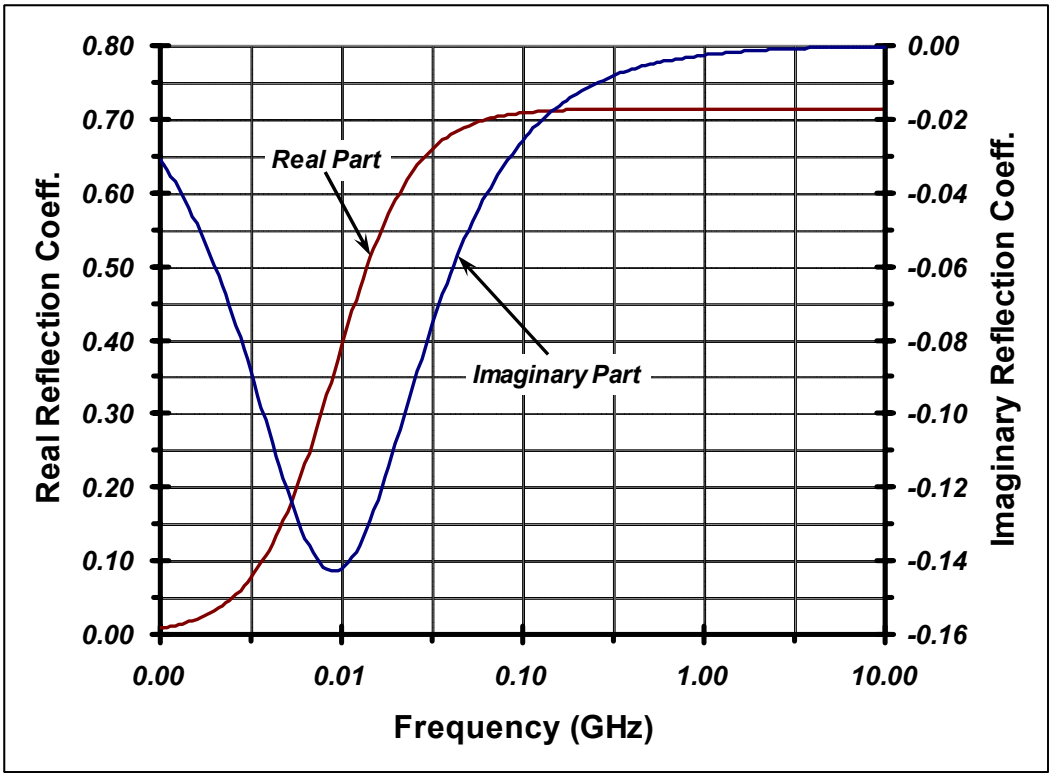


**Fig. (6).** The Real Part And The Imaginary Part Components Of The Reflection Coefficient Associated With The Impedance Established By The Simple RC Filter In Figure (5). The Circuit Resistance, $R$, Is *300 Ω*, The Circuit Capacitance, $C$, Is *50 pF*, And The Reference Impedance, $R_o$, Is *50 Ω*.

**COMMENTS:** In Figure (6), the imaginary component of the load reflection coefficient is minimized at $X_{lno} = -(R_{ln} + 1) = -(R_l + R_o)/R_o = -7$. The corresponding signal frequency, $\omega_o$, is

$$\omega_o = \frac{1}{(R_l + R_o)C},$$

which is the *3-dB* bandwidth of the circuit offered in Figure (5b). Specifically, the subject frequency is the *3-dB* bandwidth of the lowpass circuit formed by driving the load impedance undergoing examination with a signal voltage source whose Thévenin resistance is identical to the reference impedance used in the course of impedance characterization.

## EXAMPLE #2:

Plot the real and imaginary parts of the reflection coefficient, as a function of signal frequency, for the impedance established by the RLC network in Figure (7a). In the course of plotting these reflection coefficient components, normalize the signal frequency to the center frequency, $\omega_o$, of the impedance function. The indicated series circuit resistance, $R$, is *300 Ω*, while the quality factor, $Q$, of the RLC impedance is *3*. The reference impedance $(R_o)$ is *50 Ω*.

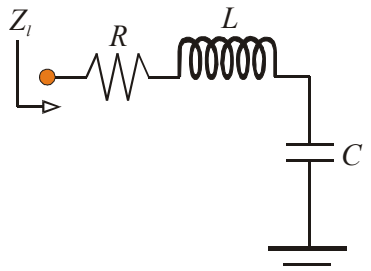


**Fig. (7).** Series RLC Bandpass Filter Addressed In Example #2.

## SOLUTION:

**(1).** The impedance of the RLC network in Figure (7a) is

$$Z_l = R + j\omega L + \frac{1}{j\omega C},$$

which is equivalent to

$$Z_l = R + jQR\left(\frac{\omega}{\omega_o} - \frac{\omega_o}{\omega}\right).$$

In the last expression,

$$\omega_o = \frac{1}{\sqrt{LC}}$$

is the resonant frequency (in radians -per- second) of the impedance, while

$$Q = \frac{\omega_o L}{R} = \frac{\sqrt{L/C}}{R}$$

is the quality factor of the impedance.

**(2).** The normalized load resistance, $R_{ln}$, follows as

$$R_{ln} = \frac{R}{R_o},$$

and the normalized reactive component of this load impedance is

$$X_{ln} = Q\frac{R}{R_o}\left(\frac{\omega}{\omega_o}-\frac{\omega_o}{\omega}\right) = QR_{ln}\left(\frac{\omega}{\omega_o}-\frac{\omega_o}{\omega}\right).$$

The foregoing two analytical results can now be substituted into (25) and (26) to generate the plots provided in Figure (8).

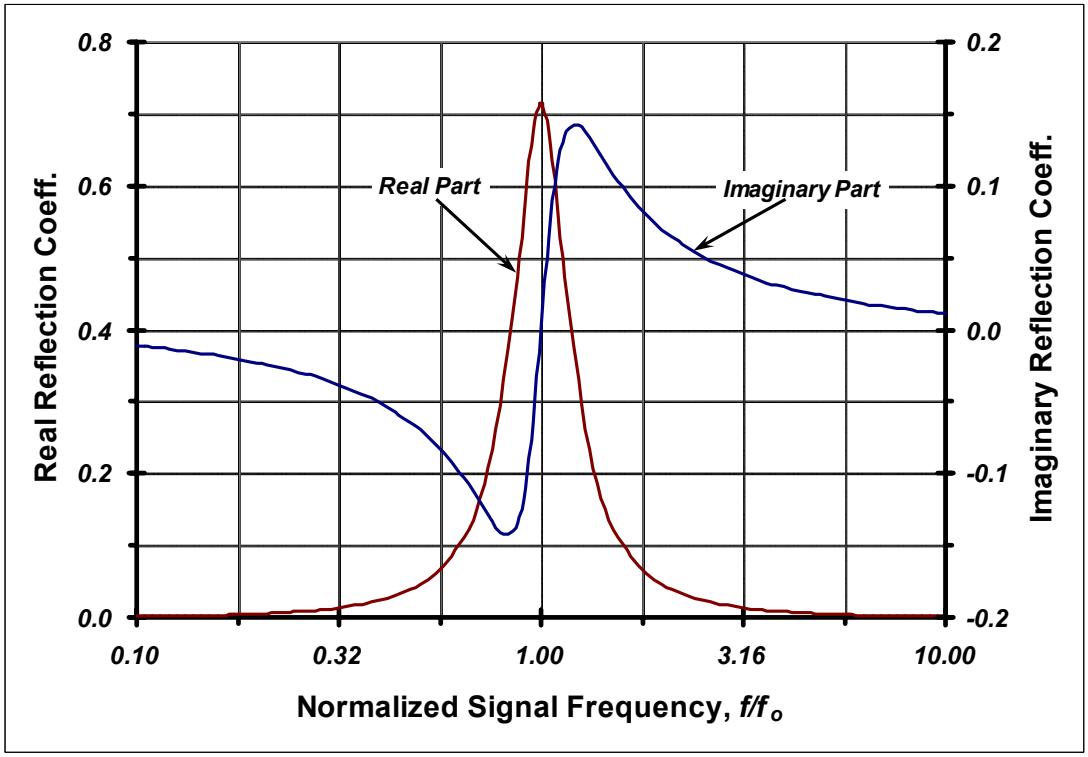


**Fig. (8).** The Real Part And The Imaginary Part Components Of The Reflection Coefficient Associated With The Impedance Established By The Filter In Figure (7). The Circuit Resistance, $R$, Is $300\ \Omega$, The Impedance Quality Factor, $Q$, Is $3$, And The Reference Impedance, $R_o$, Is $50\ \Omega$.

**COMMENTS:** As expected, the imaginary part of the reflection coefficient vanishes at the resonant frequency (at $\omega/\omega_o = 1$), since this imaginary reflection parameter is directly proportional to the effective reactance of the considered impedance. At signal frequencies that are smaller than the resonant frequency, where the impedance is dominantly capacitive, the imaginary reflection component is negative, analogous to the disclosures offered in the preceding example. On the other hand, $\rho_i$ is understandably positive for $\omega > \omega_o$, where the impedance is dominated by circuit inductance. The indicated peaks in the $\rho_i$–profile occur at frequency values that satisfy (27). It can be shown that the frequency difference, say $\Delta\omega_o$, between these observed maxima is a measure of the impedance quality factor and specifically,

$$\Delta\omega_o = \frac{1}{Q}\left(1+\frac{1}{R_{ln}}\right).$$

Finally, note the $\rho_r$, the real part component of the reflection coefficient, is maximized at the resonant frequency, where $\rho_i = 0$. Since $\rho_i = 0$ is in one -to- one correspondence with $X_{ln} = 0$, this maximum real part reflection coefficient is, from (25),

$$\rho_{rmax} = \frac{R_{ln} - 1}{R_{ln} + 1}.$$

In other words, for a given reference impedance, $R_o$, the measurement of $\rho_{rmax}$ is tantamount to a measurement of $R$, the resistance appearing in series with the inductor. This observation is often exploited gainfully in the determination of the parasitic resistance that unavoidably appears in series with circuit inductance.

# 3.0. TWO PORT SCATTERING PARAMETERS

The concept of the reflection coefficient, which is essentially the lone scattering parameter of a one port linear network, serves as an expedient springboard to the scattering parameter characterization and analysis of linear two port networks. To this end, consider the abstraction in Figure (9), which depicts a linear two port network to which test sinusoidal voltages, $V_{s1}$ and $V_{s2}$, are applied to the input and output ports, respectively. It is critical to observe that the series impedances associated with these two test voltages are identical. These resistances, which are symbolized as $R_o$, are the known reference impedances to which the network at hand is undergoing an input/output (I/O) port characterization. Invariably, $R_o$ is *50 ohms* and in such a case, the network under test is said to be undergoing a characterization in a *50 Ω* test fixture or a *50 Ω* test environment.

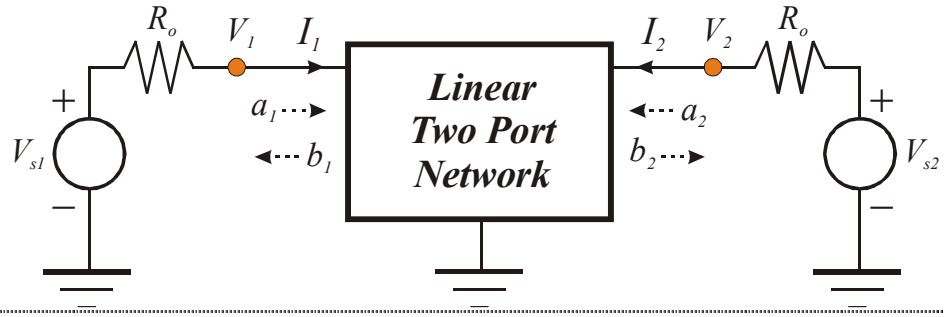


**Fig. (9).** Abstraction Of A Linear Two Port System Undergoing A Scattering Parameter Characterization In A Test Environment Whose Reference Impedance Is $R_o$. The $a_i$ Denote Incident Energy Waves At The Network Ports, While The $b_i$ Are Reflected Energy Waves At The System Ports.

The indicated port voltages, $V_1$, and $V_2$, which are established in response to the applied test signals, $V_{s1}$ and $V_{s2}$, can be viewed respectively as a superposition of incident and reflected components. Following the lead of (8),

$$\left.\begin{aligned} V_1 &= V_{1i} + V_{1r} \\ V_2 &= V_{2i} + V_{2r} \end{aligned}\right\rangle, \tag{29}$$

where the incident component, $V_{1i}$, of input port voltage $V_1$ is simply $V_{s1}/2$, and $V_{2i}$, the incident component of output port voltage $V_2$, is $V_{s2}/2$. The immediate effect of test signal $V_{s1}$ is the application of energy to the input port of the network. When the driving point network input impedance is matched to the reference impedance, $R_o$, maximum energy transfer from $V_{s1}$ -to-the input port occurs. This maximal energy is symbolized in the figure as the incident energy wave, $a_1$. Since the input impedance is generally not matched to the reference impedance, the actual energy transferred is smaller than $a_1$. The resultant difference between $a_1$ and the actual

energy transferred is the reflected input port energy wave, which is denoted in the figure as $b_1$. Analogous statements can be proffered for the incident and reflected energy waves, $a_2$, and $b_2$, respectively, that prevail at the network output port. These $a_i$ and $b_i$ are written as

$$\left.\begin{aligned} a_1 &= V_{1i}\Big/\sqrt{R_o} = \sqrt{R_o}\, I_{1i} \\ a_2 &= V_{2i}\Big/\sqrt{R_o} = \sqrt{R_o}\, I_{2i} \end{aligned}\right\rangle \tag{30}$$

and

$$\left.\begin{aligned} b_1 &= V_{1r}\Big/\sqrt{R_o} = \sqrt{R_o}\, I_{1r} \\ b_2 &= V_{2r}\Big/\sqrt{R_o} = \sqrt{R_o}\, I_{2r} \end{aligned}\right\rangle, \tag{31}$$

where (12) and (13) have been utilized. These seemingly strange algebraic relationships are placed in proper engineering perspective when it is noted that the square magnitudes of the various $a_i$ and $b_i$ respectively represent incident and reflected port power levels.

The scattering parameters, $S_{ij}$, of the two port network under consideration can now be introduced in the context of the matrix relationship,

$$\begin{bmatrix} b_1 \\ b_2 \end{bmatrix} = \begin{bmatrix} S_{11} & S_{12} \\ S_{21} & S_{22} \end{bmatrix} \begin{bmatrix} a_1 \\ a_2 \end{bmatrix}. \tag{32}$$

The definition and the measurement of these four scattering parameters proceed directly from this defining relationship. But unlike conventional two port parameters, considerable engineering care must be exercised to ensure the accurate and meaningful interpretation of these parametric definitions.

To begin, note that under the condition of $a_2 = 0$,

$$\left.\begin{aligned} S_{11} &= \left.\frac{b_1}{a_1}\right|_{a_2=0} \\ S_{21} &= \left.\frac{b_2}{a_1}\right|_{a_2=0} \end{aligned}\right\rangle. \tag{33}$$

The constraint, $a_2 = 0$, implies zero signal incidence at the output port of the network under test. Since the output port in Figure (9) is driven by a test signal, $V_{s2}$, placed in series with the measurement reference impedance, $R_o$, of the system, $a_2 = 0$ is equivalent to the constraint, $V_{s2} = 0$. This assertion derives from the general observation that energy incidence at the network output port materializes from only two sources. The first and most obvious of these two sources is purposefully applied output port energy in the form of the signal voltage, $V_{s2}$, which is nulled in this particular exercise. The second of these sources is signal reflection from the load impedance. But such reflection is zero when the load impedance is identical to the measurement reference impedance of the system. Accordingly, $a_2$ is held fast at zero precisely because $V_{s2}$ is set to zero and the terminating load impedance at the output port is $R_o$.

From (30) and (31), $S_{11}$ in (33) is equivalent to

$$S_{11} = \left.\frac{b_1}{a_1}\right|_{a_2=0} = \left.\frac{V_{1r}}{V_{1i}}\right|_{a_2=0} . \tag{34}$$

Recalling (10) and the fact that $a_2 = 0$ implies an exclusively passive load termination in the reference impedance, $R_o$, $S_{11}$ is seen as the input port reflection coefficient under the special circumstance of an output port terminated in the characteristic impedance of the measurement fixture. Letting $Z_{in}(R_o)$ denote this specialized input impedance, where the parenthesized $R_o$ underscores the requisite output port load,

$$S_{11} = \frac{Z_{in}(R_o) - R_o}{Z_{in}(R_o) + R_o} = \frac{Z_{in}(R_o)/R_o - 1}{Z_{in}(R_o)/R_o + 1} . \tag{35}$$

It is imperative to understand that the input port impedance, $Z_{in}(R_o)$, in (35) is not the driving point input impedance of the network identified for characterization; that is, it is <u>not</u> the input impedance under actual load circumstances. Instead, it is the input impedance under the condition of a load impedance set equal to the reference impedance of the test fixture. Figure (10a) attempts to underscore this observation.

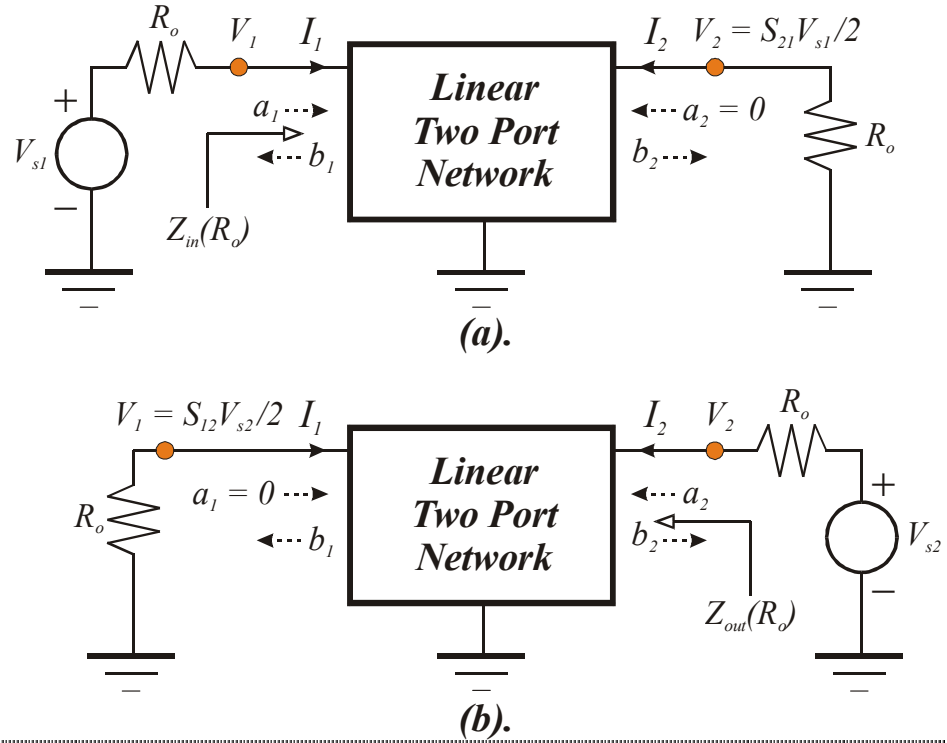


**Fig. (10).** **(a).** Test Fixturing For The Measurement Of The Scattering Parameters, $S_{11}$ And $S_{21}$, Of A Linear Two Port Network. **(b).** Test Fixturing For The Measurement Of $S_{22}$ And $S_{12}$.

Returning to (30), (31), and (33) once again,

$$S_{21} = \left.\frac{b_2}{a_1}\right|_{a_2=0} = \left.\frac{V_{2r}}{V_{1i}}\right|_{a_2=0} = 2\frac{V_2}{V_{s1}} , \tag{36}$$

where use has been made of the facts that zero energy incidence at the output port means that the output port voltage, $V_2$, is solely a reflected component voltage, $V_{2r}$, and $V_{1i} \equiv V_{s1}/2$. As is con-

firmed in Figure (10a), parameter $S_{21}$ is seen as simply twice the voltage gain under the conditions of a Thévenin source impedance of $R_o$ and an output load impedance likewise equal to $R_o$. It is also interesting to note that the squared magnitude of parameter $S_{21}$ is intimately related to the signal power gain of the subject network. In particular,

$$|S_{21}|^2 = \left|2\frac{V_2}{V_{s1}}\right|^2 = \frac{|V_2|^2/R_o}{|V_{s1}|^2/4R_o}. \tag{37}$$

The numerator on the right hand side of this relationship is clearly the power delivered by the network output port to the reference impedance load of $R_o$. On the other hand, the denominator on the right hand side of (37) represents the maximum possible power deliverable by the signal source applied at the input port. Thus, when the network at hand is terminated at its output port in $R_o$ and driven at its input port by a signal source whose Thévenin equivalent resistance is $R_o$, the squared magnitude of $S_{21}$ is simply the ratio of delivered output power -to- maximum available source power. This ratio is termed the transducer power gain, $G_T$, of a linear network; that is,

$$|S_{21}|^2 = \frac{|V_2|^2/R_o}{|V_{s1}|^2/4R_o} = 4\left|\frac{V_2}{V_{s1}}\right|^2 \triangleq G_T . \tag{38}$$

It is worthwhile interjecting parenthetically that the frequency response of the transducer power gain of an active network generally provides a more meaningful illumination of circuit frequency response than does either the current gain of a device or the voltage or current gain of a circuit. This statement derives from the simple fact that active networks are generally utilized for the explicit purpose of boosting signal power gain, as opposed to providing current or voltage amplification. In a lowpass system therefore, the signal frequency at which the transducer power gain degrades from its low frequency value by *6-dB* is a more realistic measure of high frequency circuit properties than is either the traditional unity gain frequency of a device or the *3-dB* bandwidth of circuit current or voltage gain.

Parameters $S_{22}$ and $S_{12}$ are defined in fashions analogous to the definitions of $S_{11}$ and $S_{21}$. From (32),

$$\left.\begin{aligned} S_{22} &= \left.\frac{b_2}{a_2}\right|_{a_1=0} \\ S_{12} &= \left.\frac{b_1}{a_2}\right|_{a_1=0} \end{aligned}\right\rangle . \tag{39}$$

The condition of zero input port energy incidence, $a_1 = 0$, is equivalent to the stipulations of a zero input signal source, $V_{s1} = 0$, and an input port terminated to signal ground through the reference impedance, $R_o$. Accordingly, $S_{22}$ is the corresponding reflection coefficient of the output port,

$$S_{22} = \frac{Z_{out}(R_o) - R_o}{Z_{out}(R_o) + R_o} = \frac{Z_{out}(R_o)/R_o - 1}{Z_{out}(R_o)/R_o + 1}, \tag{40}$$

where, as is inferred in Figure (10b), $Z_{out}(R_o)$ specifies the output port impedance measured under the condition of a match terminated input port. Moreover, and under the same termination circumstances, $S_{12}$ is related to the reverse, or feedback, voltage gain of the network. Specifically,

$$S_{12} = \left.\frac{b_1}{a_2}\right|_{a_1=0} = \left.\frac{V_{1r}}{V_{2i}}\right|_{a_1=0} = 2\frac{V_1}{V_{s2}}. \tag{41}$$

A final noteworthy observation derives from (29) -through- (31). In particular, the input and output port voltages, $V_1$ and $V_2$, respectively, can be written as

$$\left.\begin{aligned} V_1 &= \sqrt{R_o}\,(a_1 + b_1) \\ V_2 &= \sqrt{R_o}\,(a_2 + b_2) \end{aligned}\right\rangle. \tag{42}$$

Since currents are expressed as a difference between incident and reflected components, (30) and (31) also confirm that

$$\left.\begin{aligned} I_1 &= \frac{a_1 - b_1}{\sqrt{R_o}} \\ I_2 &= \frac{a_2 - b_2}{\sqrt{R_o}} \end{aligned}\right\rangle. \tag{43}$$

It follows that short circuited linear network ports, which are required in the measurement of the admittance parameters, require $a_i = -b_i$. On the other hand open circuited ports, which are demanded of impedance parameter extraction, mandate $a_i = b_i$.

## 3.1. SCATTERING ANALYSIS OF A GENERALIZED TWO PORT

Figure (11) abstracts the general case of a linear two port network undergoing an I/O characterization in the sinusoidal steady state. The signal source applied at the input port of the network is represented as a Thévenin equivalent circuit whose voltage is $V_s$ and whose impedance is $Z_s$. The output port of the subject linear network is terminated to ground through an impedance of $Z_l$. The two port network itself is presumed to have scattering parameters, $S_{ij}$, extracted with respect to a known real reference impedance, $R_o$. Accordingly, the indicated I/O incident and reflected energy waves, $a_1$, $b_1$, $a_2$, and $b_2$, subscribe to (32). It is also assumed that the source and load impedances are measured indirectly as source and load reflection coefficients, $\rho_s$ and $\rho_l$, referenced as well to $R_o$. Thus, the incident and reflected energy waves, $a_s$ and $b_s$, pertinent to the source termination satisfy the relationship,

$$\rho_s = \frac{b_s}{a_s} = \frac{Z_s - R_o}{Z_s + R_o}. \tag{44}$$

Similarly, for the output port,

$$\rho_l = \frac{b_l}{a_l} = \frac{Z_l - R_o}{Z_l + R_o}. \tag{45}$$

Since no signal energy source is explicitly applied at the output port as an independent voltage or current source, the energy wave, $a_2$, incident at the output port of the linear network is necessar-

ily equal to the energy reflected back to said port by the load impedance; that is, $a_2 = b_l$. Additionally, all energy reflected at the output port of the linear network is incident to the load impedance, thereby establishing the constraint, $b_2 = a_l$. It follows that the output port reflection coefficient, $\rho_2$, relates to the load reflection coefficient, $\rho_l$, as

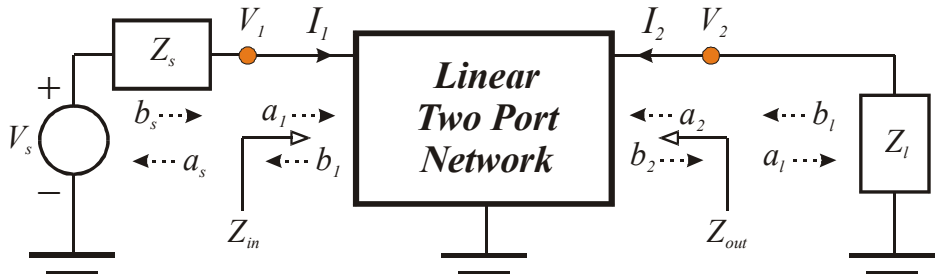


**Fig. (11).** Linear Network Terminated At Its Input And Output Ports In Generalized Load And Source Impedances. The Two Port Network Is Presumed To Have Measured Or Otherwise Known Scattering Parameters Referenced To A Characteristic Impedance Of $R_o$.

$$\rho_2 = \frac{b_2}{a_2} = \frac{a_l}{b_l} = \frac{1}{\rho_l} . \tag{46}$$

### 3.1.1. Input and Output Port Reflection Coefficients

The determination of the reflection coefficient for the input port of the subject linear two port network is tantamount to determining the driving point input impedance, $Z_{in}$; that is, the input impedance under actual load termination conditions. Since $b_2 = a_l$ and $a_2 = b_l = \rho_l a_l$ in Figure (11), (32) yields

$$a_l = S_{21}a_1 + S_{22}b_l = S_{21}a_1 + \rho_l S_{22}a_l ,$$

or

$$a_l = \left(\frac{S_{21}}{1-\rho_l S_{22}}\right) a_1 . \tag{47}$$

Returning once again to (32),

$$b_l = S_{11}a_1 + S_{12}a_2 = S_{11}a_1 + S_{12}b_l = S_{11}a_1 + \rho_l S_{12}a_l . \tag{48}$$

Upon substitution of (47) into (48), the reflection coefficient, $\rho_1$, of the input port is seen to be

$$\rho_1 = \frac{b_1}{a_1} = S_{11} + \frac{\rho_l S_{12}S_{21}}{1-\rho_l S_{22}} . \tag{49}$$

Three noteworthy observations surface from the preceding analytical result. First, note that $\rho_1 = S_{11}$ when $\rho_l = 0$, which defines a load impedance matched to the reference impedance $(Z_l = R_o)$. This result is expected in view of the fact that $S_{11}$ is, by definition, the input port reflection coefficient under the special case of a load termination matched to the reference impedance. Second, $\rho_1 = S_{11}$ even if $\rho_l \neq 0$, provided $S_{12} = 0$. The constraint, $S_{12} = 0$, equates to a zero feedback condition for the linear two port at hand. In turn, zero feedback isolates the input port from the output port, which means that the input impedance is independent of the terminating load impedance. Equivalently, the input port reflection coefficient is unaffected by

load reflections, thereby rendering an input port reflection coefficient identical to $S_{11}$, which represents the input port reflection coefficient for null reflected load energy. Finally, since

$$\rho_1 \;=\; \frac{b_1}{a_1} \;=\; \frac{Z_{in}-R_o}{Z_{in}+R_o}\;, \tag{50}$$

(49) uniquely stipulates the network driving point impedance in accordance with

$$Z_{in} \;=\; \left(\frac{1+\rho_1}{1-\rho_1}\right)R_o \;=\; \left[\frac{\left(1-\rho_l S_{22}\right)\left(1+S_{11}\right)+\rho_l S_{12}S_{21}}{\left(1-\rho_l S_{22}\right)\left(1-S_{11}\right)-\rho_l S_{12}S_{21}}\right]R_o\;. \tag{51}$$

Analyses that mirror the foregoing documentation leads forthwith to an expression for the output port reflection coefficient, $\rho_2$. In particular, it can be shown that

$$\rho_2 \;=\; \frac{b_2}{a_2} \;=\; \frac{Z_{out}-R_o}{Z_{out}+R_o} \;=\; S_{22} \;+\; \frac{\rho_s S_{12}S_{21}}{1-\rho_s S_{22}}\;, \tag{52}$$

which defines the driving point output impedance, $Z_{out}$, as

$$Z_{out} \;=\; \left(\frac{1+\rho_2}{1-\rho_2}\right)R_o \;=\; \left[\frac{\left(1-\rho_s S_{11}\right)\left(1+S_{22}\right)+\rho_s S_{12}S_{21}}{\left(1-\rho_s S_{11}\right)\left(1-S_{22}\right)-\rho_s S_{12}S_{21}}\right]R_o\;. \tag{53}$$

For reasons entirely analogous to those provided in conjunction with the input port reflection coefficient, $\rho_2 = S_{22}$ when either $\rho_s$ or $S_{12}$ (or both) are zero.

### 3.1.2. Voltage Transfer Function

In Figure (11), the input port -to- output port voltage transfer function is the voltage ratio, $V_2/V_1$, which from (42) is

$$\frac{V_2}{V_1} \;=\; \frac{a_2+b_2}{a_1+b_1} \;=\; \frac{a_2}{a_1}\left(\frac{1+\rho_2}{1+\rho_1}\right). \tag{54}$$

The energy ratio, $a_2/a_1$, in this relationship can be expressed in terms of measurable parameters by returning to (32). In particular,

$$b_2 \;=\; S_{21}a_1 + S_{22}a_2 \;=\; \rho_2 a_2\;, \tag{55}$$

from which,

$$\frac{a_2}{a_1} \;=\; \frac{S_{21}}{\rho_2 - S_{22}}\,. \tag{56}$$

Inserting (56) into (54) and using (46), the I/O port voltage transfer function becomes

$$\frac{V_2}{V_1} \;=\; \frac{S_{21}}{1-\rho_l S_{22}}\left(\frac{1+\rho_l}{1+\rho_1}\right). \tag{57}$$

Now, the input port voltage, $V_1$, is related to the signal source voltage, $V_s$, through the simple voltage divider expression,

$$\frac{V_1}{V_s} = \frac{Z_{in}}{Z_{in}+Z_s} . \tag{58}$$

In terms of pertinent reflection coefficients, this divider is

$$\frac{V_1}{V_s} = \frac{Z_{in}}{Z_{in}+Z_s} = \frac{\dfrac{1+\rho_1}{1-\rho_1}}{\dfrac{1+\rho_1}{1-\rho_1}+\dfrac{1+\rho_s}{1-\rho_s}} = \frac{(1+\rho_1)(1-\rho_s)}{2(1-\rho_1\rho_s)} . \tag{59}$$

Since the overall voltage transfer function, $A_v$, is

$$A_v \triangleq \frac{V_2}{V_s} = \frac{V_2}{V_1}\times\frac{V_1}{V_s} , \tag{60}$$

(57), (59), and (49), combine to deliver

$$A_v = \frac{V_2}{V_s} = \frac{S_{21}}{2}\left[\frac{(1-\rho_s)(1+\rho_l)}{(1-\rho_s S_{11})(1-\rho_l S_{22})-\rho_s\rho_l S_{12}S_{21}}\right]. \tag{61}$$

In an attempt to make sense of the algebraic garble that defines the system voltage transfer function in terms of measured two port network scattering parameters and measured source and load reflection coefficients, note in (61) that when $\rho_s = \rho_l = 0$, $A_v$ collapses to $S_{21}/2$. This result corroborates with an earlier disclosure that postures $S_{21}$ as twice the forward voltage gain of a network terminated at its output port in the reference impedance and driven at its input port by a Thévenin equivalent source resistance that likewise equals the system reference impedance. Under such an operational circumstance, $S_{21}$ as a viable measure of forward gain capabilities. Moreover, when the I/O ports are reasonably reference-terminated in the senses that $Z_s \approx R_o$ and $Z_l \approx R_o$ to render $\rho_s \approx 0$ and $\rho_l \approx 0$, the frequency response of $S_{21}$ becomes a meaningful measure of the achievable system frequency response.

A second observation is that for the case of zero internal feedback, the resultant voltage gain, which can rightfully be termed the open loop gain, say $A_{vo}$, of the system, is

$$A_{vo} = A_v\big|_{S_{12}=0} = \frac{S_{21}(1-\rho_s)(1+\rho_l)}{2(1-\rho_s S_{11})(1-\rho_l S_{22})} . \tag{62}$$

It is convenient to write this open loop gain in the form,

$$A_{vo} = (1-\rho_s)(1+\rho_l)A_{ve} , \tag{63}$$

where

$$A_{ve} = \frac{S_{21}}{2(1-\rho_s S_{11})(1-\rho_l S_{22})} . \tag{64}$$

Resultantly, (61) is expressible as

$$A_v = (1-\rho_s)\left(\frac{A_{ve}}{1-2\rho_s\rho_l S_{12}A_{ve}}\right)(1+\rho_l) , \tag{65}$$

where an effective loop gain, $T$, of

$$T = -2\rho_s\rho_l S_{12} A_{ve} \tag{66}$$

is immediately transparent. Equation (65) gives rise to the block diagram representation offered in Figure (12), where the factors, $(1-\rho_s)$ and $(1+\rho_l)$ in this diagram and in (65) account for the cognizant effects of impedance mismatches at the input and output ports, respectively.

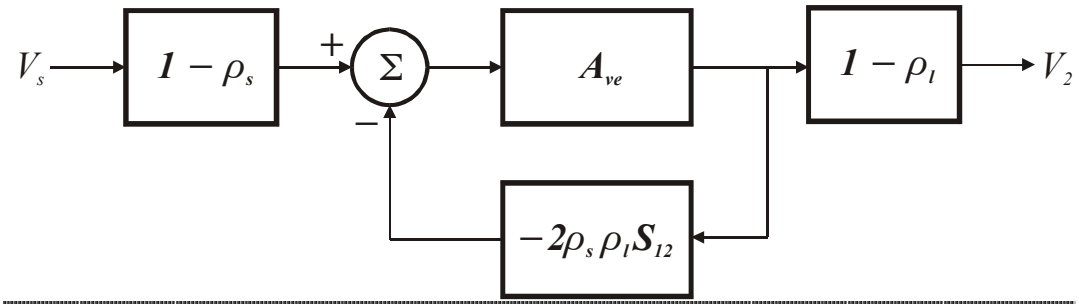


**Fig. (12).** Block Diagram Model Of The Scattering Parameter Voltage Transfer Relationship For The Generalized Linear System Offered In Figure (11).

### 3.1.3. Other Transfer Functions

The voltage transfer function in (61) serves as an analytical foundation for the determination of other types of I/O relationships, such as transadmittance, transimpedance, and current gain. For example, the linear configuration in Figure (11) confirms $V_2 = -I_2 Z_l$, whence

$$A_v = \frac{V_2}{V_s} = -\frac{I_2 Z_l}{V_s}. \tag{67}$$

It follows that the forward transadmittance, $Y_f$, is

$$Y_f = \frac{I_2}{V_s} = -\frac{A_v}{Z_l}. \tag{68}$$

Substituting (45) for the load impedance, $Z_l$, (68) and (61) combine to deliver a normalized forward transadmittance of

$$Y_f R_o = -\frac{S_{21}}{2}\left[\frac{(1-\rho_s)(1-\rho_l)}{(1-\rho_s S_{11})(1-\rho_l S_{22})-\rho_s\rho_l S_{12}S_{21}}\right]. \tag{69}$$

The relationships for current gain and transimpedance can be similarly constructed.

## 3.2. SCATTERING PARAMETERS RELATED TO CONVENTIONAL TWO PORT PARAMETERS

Since the scattering parameters of a linear two port network serve to define its terminal I/O and transfer characteristics, these parameters must be consistent with conventional two port parameters (admittance, impedance, hybrid h–, and hybrid g–), which also delineate the I/O and transfer properties of a linear system. Consider, for example, the network in Figure (11) modeled by the h–parameter equivalent circuit provided in Figure (13). On the assumption that the desired S–parameters are to be referred to a characteristic impedance of $R_o$, care has been exercised in Figure (13) to terminate both the input and output ports in $R_o$.

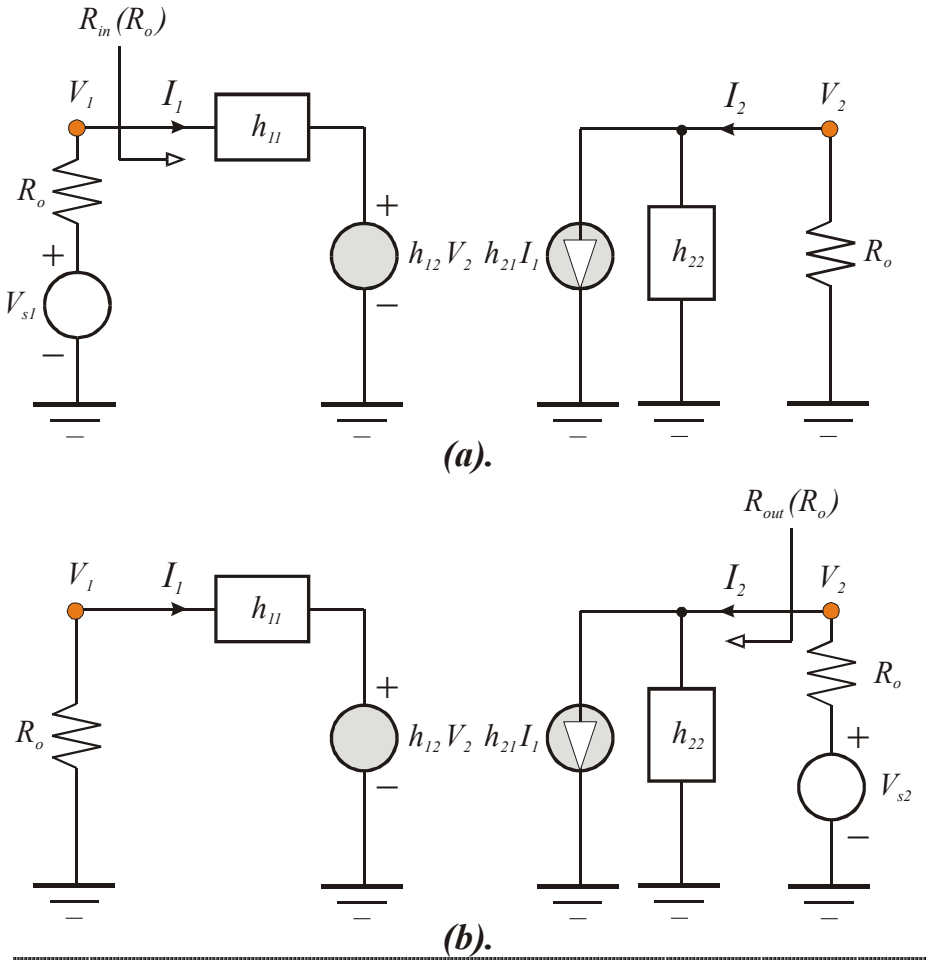


**Fig. (13).** **(a).** The h–Parameter Model Of The Linear Network In Figure (11) Used In The Determination Of The Input Impedance And Forward Voltage Gain With The Output Port Terminated In The Characteristic Impedance, $R_o$. **(b).** The Model Of (a) Configured For The Evaluation Of The Output Impedance And Reverse (Or Feedback) Voltage Gain With The Input Port Terminated In $R_o$.

An inspection of Figure (13a) reveals a reference-terminated input impedance of

$$Z_{in}(R_o) = h_{11} - \frac{h_{12}h_{21}R_o}{1+h_{22}R_o} \tag{70}$$

and a reference-driven, reference-terminated voltage gain of

$$A_v(R_o) = \frac{V_2}{V_{s1}} = -\frac{h_{21}R_o}{(h_{11}+R_o)(1+h_{22}R_o) - h_{12}h_{21}R_o}. \tag{71}$$

Equations (70) and (35) produce an input port scattering parameter, $S_{11}$, of

$$S_{11} = \frac{(h_{11}-R_o)(1+h_{22}R_o) - h_{12}h_{21}R_o}{(h_{11}+R_o)(1+h_{22}R_o) - h_{12}h_{21}R_o}, \tag{72}$$

while (71) and (36) combine to deliver

$$S_{21} = -\frac{2h_{21}R_o}{(h_{11}+R_o)(1+h_{22}R_o) - h_{12}h_{21}R_o}. \tag{73}$$

As expected, the scattering parameter, $S_{21}$, which is a measure of achievable forward gain, is nominally proportional to h–parameter $h_{21}$. If negligible feedback $(h_{12} \approx 0)$ prevails within the network undergoing characterization, parameter $S_{21}$ is simply twice the open loop voltage gain, while $S_{11}$ in (72) reduces to

$$S_{11} \approx \frac{h_{11}-R_o}{h_{11}+R_o}. \tag{74}$$

The last expression correctly infers an input impedance, $h_{11}$, that is independent of load termination when negligible internal feedback is evidenced.

In Figure (13b), the output impedance under the condition of the input port terminated to ground through the reference impedance, $R_o$, derives from

$$\frac{1}{Z_{out}(R_o)} = h_{22} - \frac{h_{12}h_{21}R_o}{h_{11}+R_o}, \tag{75}$$

whence, by (40),

$$S_{22} = \frac{(h_{11}+R_o)(1-h_{22}R_o) + h_{12}h_{21}R_o}{(h_{11}+R_o)(1+h_{22}R_o) - h_{12}h_{21}R_o}. \tag{76}$$

For the case of negligible feedback,

$$S_{22} \approx \frac{1-h_{22}R_o}{1+h_{22}R_o} = \frac{\frac{1}{h_{22}} - R_o}{\frac{1}{h_{22}} + R_o}, \tag{77}$$

which properly casts $1/h_{22}$ as the output impedance established under zero feedback conditions. A straightforward analysis of the same circuit diagram also confirms a reverse voltage gain of

$$\frac{V_1}{V_{s2}} = \frac{h_{12}R_o}{(h_{11}+R_o)(1+h_{22}R_o) - h_{12}h_{21}R_o}, \tag{78}$$

which, by (41), infers a feedback S–parameter, $S_{12}$, of

$$S_{12} = \frac{2h_{12}R_o}{(h_{11}+R_o)(1+h_{22}R_o) - h_{12}h_{21}R_o}. \tag{79}$$

Observe that $S_{12}$ vanishes if the network offers no internal feedback $(h_{12} = 0)$. Additionally, (79) and (73) show that

$$\frac{S_{21}}{S_{12}} = -\frac{h_{21}}{h_{12}}, \tag{80}$$

which ensures $S_{21} \equiv S_{12}$ for a passive, and hence bilateral, linear network.

## 3.3. CONVENTIONAL TWO PORT PARAMETERS RELATED TO SCATTERING PARAMETERS

Because of previously noted difficulties with regard to maintaining reliable and accurate short circuited and open circuited network ports at high signal frequencies, the conventional two port parameters of passive and active linear devices, circuits, and systems earmarked for high frequency signal processing applications are invariably deduced indirectly via scattering parameters. Moreover, and as is illuminated in the preceding section of material, the analytical expressions that define the electrical nature of the two port driving point and transfer characteristics in terms of S–parameters are somewhat cumbersome and therefore challenging to interpret insightfully from a design perspective. It follows that relating the conventional two port parameters explicitly to S–parameters is a warranted task, which is undertaken herewith for the hybrid h–parameters.

The h–parameters, $h_{11}$ and $h_{21}$, for a linear two port network such as the one abstracted in Figure (13), are evaluated under the condition of a short circuited output port; that is, $V_2 = 0$. From (42), $V_2 = 0$ implies $a_2 = -b_2$, which means that the incident output port variable is the negative of its reflected counterpart or equivalently, the output port reflection coefficient, $\rho_2$, is negative one. Recalling (32), $a_2 = -b_2$ delivers

$$a_2\big|_{a_2=-b_2} = -\left(\frac{S_{21}}{1+S_{22}}\right)a_1 \ , \tag{81}$$

$$b_1 = S_{11}a_1 + S_{12}a_2 = S_{11}a_1 - \left(\frac{S_{12}S_{21}}{1+S_{22}}\right)a_1 \ ,$$

and a resultant input port reflection coefficient of

$$\rho_1 = \left.\frac{b_1}{a_1}\right|_{a_2=-b_2} = S_{11} - \frac{S_{12}S_{21}}{1+S_{22}} \ . \tag{82}$$

From (42) and (43),

$$h_{11} \triangleq \left.\frac{V_1}{I_1}\right|_{V_2=0} = \left.\frac{R_o\left(a_1+b_1\right)}{a_1-b_1}\right|_{a_2=-b_2} = R_o\left.\left(\frac{1+\rho_1}{1-\rho_1}\right)\right|_{a_2=-b_2} \ . \tag{83}$$

Upon combining (82) and (83),

$$\frac{h_{11}}{R_o} = \frac{\left(1+S_{11}\right)\left(1+S_{22}\right) - S_{12}S_{21}}{\left(1-S_{11}\right)\left(1+S_{22}\right) + S_{12}S_{21}} \ . \tag{84}$$

While maintaining $V_2 = 0$ or equivalently, $a_2 = -b_2$, (43) assists in casting the short circuit current gain, $h_{21}$, in the form

$$h_{21} = \left.\frac{I_2}{I_1}\right|_{V_2=0} = \left.\frac{a_2-b_2}{a_1-b_1}\right|_{a_2=-b_2} = \left.\frac{a_2}{a_1}\left(\frac{2}{1-\rho_1}\right)\right|_{a_2=-b_2} \ . \tag{85}$$

Using (81) and (82), (85) becomes

$$h_{21} \;=\; -\frac{2S_{21}}{(1-S_{11})(1+S_{22}) \;+\; S_{12}S_{21}} \;. \tag{86}$$

The h–parameters, $h_{22}$ and $h_{12}$, are open circuit metrics of a linear two port network. With reference to Figure (13b), these two parameters are evaluated with the input port current, $I_1$, nulled, which is equivalent to the constraint, $a_1 = b_1$, in Figure (11). For this constraint, (32) delivers

$$a_1 \;=\; b_1 \;=\; \left(\frac{S_{12}}{1 \;-\; S_{11}}\right) a_2 \;. \tag{88}$$

Using (32) once again, the resultant open circuit reflection coefficient at the output port is

$$\rho_2 \;=\; \left.\frac{b_2}{a_2}\right|_{a_1=b_1} \;=\; S_{22} \;+\; \frac{S_{12}S_{21}}{1 \;-\; S_{11}} \;. \tag{89}$$

It follows that the open circuit output admittance, $h_{22}$, is

$$h_{22} \;\triangleq\; \left.\frac{I_2}{V_2}\right|_{I_1=0} \;=\; \left.\frac{(a_2 \;-\; b_2)}{R_o\,(a_2 \;+\; b_2)}\right|_{a_1=b_1} \;=\; \frac{1}{R_o}\left.\left(\frac{1 \;-\; \rho_2}{1 \;+\; \rho_2}\right)\right|_{a_1=b_1} \;. \tag{90}$$

Putting (89) into (90),

$$h_{22}R_o \;=\; \frac{(1 \;-\; S_{11})(1 \;-\; S_{22}) \;-\; S_{12}S_{21}}{(1 \;-\; S_{11})(1 \;+\; S_{22}) \;+\; S_{12}S_{21}} \;. \tag{91}$$

Finally, for the feedback parameter, $h_{12}$,

$$h_{12} \;=\; \left.\frac{V_1}{V_2}\right|_{I_1=0} \;=\; \left.\frac{a_1 \;+\; b_1}{a_2 \;+\; b_2}\right|_{a_1=b_1} \;=\; \frac{a_1}{a_2}\left.\left(\frac{2}{1 \;+\; \rho_2}\right)\right|_{a_1=b_1} \;. \tag{92}$$

Using (88) and (89), feedback hybrid parameter $h_{12}$ is seen to be given by

$$h_{12} \;=\; \frac{2S_{12}}{(1-S_{11})(1+S_{22}) \;+\; S_{12}S_{21}} \;. \tag{93}$$

Clearly, both $h_{12}$ and $S_{12}$ are measures of intrinsic feedback in the sense that $S_{12} = 0$ nulls $h_{12}$. The pertinent results for the foregoing four h–parameters are conveniently summarized by the hybrid h–parameter matrix,

$$\boldsymbol{h} \;=\; \begin{bmatrix} \dfrac{\{(1 \;+\; S_{11})(1 \;+\; S_{22}) \;-\; S_{12}S_{21}\}\,R_o}{(1 \;-\; S_{11})(1 \;+\; S_{22}) \;+\; S_{12}S_{21}} & \dfrac{2S_{12}}{(1 \;-\; S_{11})(1 \;+\; S_{22}) \;+\; S_{12}S_{21}} \\[2ex] \dfrac{-2S_{21}}{(1 \;-\; S_{11})(1 \;+\; S_{22}) \;+\; S_{12}S_{21}} & \dfrac{(1 \;-\; S_{11})(1 \;-\; S_{22}) \;-\; S_{12}S_{21}}{\{(1 \;-\; S_{11})(1 \;+\; S_{22}) \;+\; S_{12}S_{21}\}\,R_o} \end{bmatrix} . \tag{94}$$

# 4.0. LOSSLESS TWO PORT NETWORKS

Filters serve a plethora of purposes in electronic circuits designed for incorporation in communication systems. For example, bandpass, lowpass, notch, and other types of frequency responses are implemented to ensure that undesired signals captured at antennas and other signal source media are adequately attenuated prior to ultimately conducted signal processing. By limiting the bandwidth of filters incorporated in critical signal flow paths, the deleterious effects of noise generated by passive and active components are mitigated. Yet another filtering application is impedance matching aimed toward maximizing signal power transfer between critical source and load ports. Although a seemingly endless array of filter architectures is available to satisfy all of these, and numerous other, engineering requirements, certain pragmatic guidelines necessarily underpin the design of filters for a broad variety of high frequency or broadband radio frequency (RF) system applications.

The first of these requirements derives from the likely impropriety of adopting active network design strategies for many types of filtering requirements. One concern is the inherent frequency response shortfalls inherent to the electronic subcircuits implicit to active filter realizations. As a rule, the design of active filters for frequency operation above the mid-hundreds of megahertz comprises a daunting, if not impossible, engineering challenge. A second problem is that active filters tend to be considerably noisier than are their passive architectural counterparts. This noise issue poses a serious dilemma in low-level input stage signal processing where available signal strengths may be dangerously close to minimal electrical noise floors. Another active filter red flag that surfaces, particularly in portable electronics, is the biasing power that active elements require. Finally, active filters are not as linear as are passive architectures. This nonlinearity poses problems when input signal strength bounds are obscure and when signals of comparable amplitudes appear in proximate frequency bands to incur potentially unacceptable intermodulation responses.

Passive filter architectures circumvent many of the foregoing limitations, but they too are hardly examples of unimpeachable perfection. Component tolerances, particularly as regards resistors and capacitors, loom potentially troublesome when bandwidths or other frequency response metrics must be accurately achieved. Inductors have finite quality factors, that exacerbate circuit noise problems and limit achievable narrow band responses in bandpass circuits. Resistors associated with practical inductors and those embedded within filters incur signal power losses. This loss problem is especially serious in low-level communications that feature minimal available signal input power. No leap of faith is required to understand that if an already sparse power level is processed by an inordinately lossy filter, the resultant response at the filter output port may be substantively masked by random noise phenomena, thereby precluding reliable signal capture and accurate signal processing.

The commentary of the preceding paragraph warrants at least cursory attention to the realization of lossless, passive filters. To this end, the scattering parameter concept provides a vehicle for the development of a systematic design strategy for the realization of multiport filters whose only branch elements are either inductors or capacitors. To be sure, neither inductors or capacitors are perfectly lossless elements. But in all but the most exceptional of cases, the power losses incurred by the parasitic resistances associated with practical inductors and capacitors are far less significant than are those of branch resistances purposefully embedded in filters.

## 4.1. AVERAGE POWER DELIVERED TO COMPLEX LOAD

To begin the discussion of lossless filters, consider the simple branch impedance, $Z(j\omega)$, in Figure (14). Let this impedance conduct a steady stage sinusoidal current, $i(t)$, in response to a sinusoidal voltage, $v(t)$, established across the branch. If the subject branch voltage is

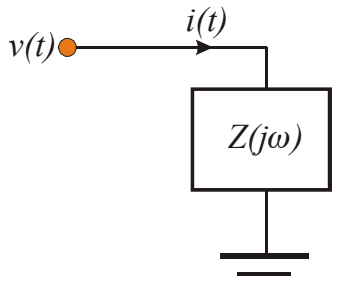


**Fig. (14).** A Complex Load Impedance To Which A Sinusoidal Voltage, $v(t)$, Is Applied And A Sinusoidal Current, $i(t)$, Resultantly Flows.

$$v(t) = \sqrt{2}\, V_m \cos(\omega t + \theta_v) \tag{95}$$

and the corresponding branch current is

$$i(t) = \sqrt{2}\, I_m \cos(\omega t + \theta_i) , \tag{96}$$

the instantaneous power, $p(t)$, delivered to the load impedance is

$$p(t) = v(t)i(t) = 2V_m I_m \cos(\omega t + \theta_v) \cos(\omega t + \theta_i) . \tag{97}$$

In (95) and (96), $V_m$ and $I_m$ respectively symbolize the root mean square (RMS) voltage and current amplitudes, while the phase difference, $(\theta_v - \theta_i)$, is the phase angle of the branch impedance. Equation (97) may be expanded to

$$p(t) = V_m I_m \left[\cos(\theta_v - \theta_i) + \cos(2\omega t + \theta_v + \theta_i)\right] , \tag{98}$$

which renders evident an average power delivery, and hence an average dissipated power, of

$$P_{avg} = \frac{1}{T}\int_0^T p(t)\, dt = V_m I_m \cos(\theta_v - \theta_i) . \tag{99}$$

Observe an average power of zero if $(\theta_v - \theta_i) = \pm 90°$, which is indicative of a purely inductive or a purely capacitive branch impedance.

An alternative, and more useful, expression for the average power dissipated by a complex load impedance is predicated on a phasor representation of the pertinent voltage and current. Specifically, write $v(t)$ and $i(t)$ in the phasor formats,

$$\left.\begin{aligned} V(j\omega) &= V_m e^{j\theta_v} \\ I(j\omega) &= I_m e^{j\theta_i} \end{aligned}\right\} . \tag{100}$$

It follows that (99) is also equivalent to writing

$$P_{avg} = Re\left[V(j\omega)I(-j\omega)\right] . \tag{101}$$

It is to be understood that $I(-j\omega)$ in the last relationship is the conjugate of the phasor, $I(j\omega)$, in (100). If the impedance, $Z(j\omega)$ is a lossless entity, which forces its phase angle for all frequencies, $\omega$, to be either positive ninety (inductive) or negative ninety (capacitive), no average power is dissipated by $Z(j\omega)$ and thus,

$$P_{avg} = Re\left[V(j\omega)I(-j\omega)\right] = 0 . \tag{102}$$

## 4.2. AVERAGE POWER DELIVERED TO TWO PORT NETWORK

The foregoing results are easily extended to embrace two port networks, such as the one that appears in Figure (11). Since the network in question has two accessible signal ports, the net power it dissipates is

$$P_{avg} = Re\left[V_1(j\omega)I_1(-j\omega) + V_2(j\omega)I_2(-j\omega)\right] . \tag{103}$$

The development of design criteria for lossless two port networks is facilitated through introduction of the port voltage and port current vectors,

$$\left.\begin{aligned} \boldsymbol{V}(j\omega) &= \begin{bmatrix} V_1(j\omega) \\ V_2(j\omega) \end{bmatrix} = \sqrt{R_o}\begin{bmatrix} a_1(j\omega) + b_1(j\omega) \\ a_2(j\omega) + b_2(j\omega) \end{bmatrix} \\ \boldsymbol{I}(j\omega) &= \begin{bmatrix} I_1(j\omega) \\ I_2(j\omega) \end{bmatrix} = \frac{1}{\sqrt{R_o}}\begin{bmatrix} a_1(j\omega) - b_1(j\omega) \\ a_2(j\omega) - b_2(j\omega) \end{bmatrix} \end{aligned}\right\rangle , \tag{104}$$

where (42) and (43) are exploited and, of course, $a_i(j\omega)$ and $b_i(j\omega)$ respectively symbolize steady state incident and reflected energy variables at the $i^{th}$ port. If the energy vectors, $\boldsymbol{a}(j\omega)$ and $\boldsymbol{b}(j\omega)$, are introduced, such that

$$\left.\begin{aligned} \boldsymbol{a}(j\omega) &= \begin{bmatrix} a_1(j\omega) \\ a_2(j\omega) \end{bmatrix} \\ \boldsymbol{b}(j\omega) &= \begin{bmatrix} b_1(j\omega) \\ b_2(j\omega) \end{bmatrix} \end{aligned}\right\rangle , \tag{105}$$

the average total power dissipated by the two port network can be related explicitly to port incident and reflected variables in accordance with

$$P_{avg} = Re\left[\boldsymbol{V}^T(j\omega)\boldsymbol{I}(-j\omega)\right] = Re\left[\left\{\boldsymbol{a}^T(j\omega) + \boldsymbol{b}^T(j\omega)\right\}\left\{\boldsymbol{a}(-j\omega) - \boldsymbol{b}(-j\omega)\right\}\right] . \tag{106}$$

The superscript *"T"* in this relationship denotes the mathematical operation of matrix transposition, where matrix rows are interchanged with matrix columns.

An interesting reduction of the average power relationship results from an expansion of the right hand side of the last equation. Specifically,

$$P_{avg} = Re\left[\boldsymbol{a}^T(j\omega)\boldsymbol{a}(-j\omega) - \boldsymbol{b}^T(j\omega)\boldsymbol{b}(-j\omega)\right] + Re\left[\boldsymbol{b}^T(j\omega)\boldsymbol{a}(-j\omega) - \boldsymbol{a}^T(j\omega)\boldsymbol{b}(-j\omega)\right] . \tag{107}$$

Because both $\boldsymbol{a}(j\omega)$ and $\boldsymbol{b}(j\omega)$ are column vectors, the matrix product, $\boldsymbol{b}^T(j\omega)\boldsymbol{a}(-j\omega)$, is a scalar. And since the transpose of a scalar is certainly the same as the scalar quantity itself,

$$\boldsymbol{b}^T(j\omega)\boldsymbol{a}(-j\omega) = \left[\boldsymbol{b}^T(j\omega)\boldsymbol{a}(-j\omega)\right]^T = \boldsymbol{a}^T(-j\omega)\boldsymbol{b}(j\omega) . \tag{108}$$

Accordingly,

$$P_{avg} = Re\left[\boldsymbol{a}^T(j\omega)\boldsymbol{a}(-j\omega) - \boldsymbol{b}^T(j\omega)\boldsymbol{b}(-j\omega)\right] + Re\left[\boldsymbol{a}^T(-j\omega)\boldsymbol{b}(j\omega) - \boldsymbol{a}^T(j\omega)\boldsymbol{b}(-j\omega)\right] . \tag{109}$$

But the first term in the second real part quantity on the right hand side of (109) is simply the complex conjugate of the second term in this real part component. Since the difference of two numbers that are complex conjugates of one another is a purely imaginary number, the second real part term in question is identically zero. Thus, the net average power dissipated by a linear two port network reduces to

$$P_{avg} = Re\left[\boldsymbol{a}^T(j\omega)\boldsymbol{a}(-j\omega) - \boldsymbol{b}^T(j\omega)\boldsymbol{b}(-j\omega)\right] . \tag{110}$$

Since each term implicit to the real part operation in this equation is a scalar formed of a product of a number and its complex conjugate, each term within the brackets is a real number, thereby allowing the average power to be simplified as

$$P_{avg} = \boldsymbol{a}^T(j\omega)\boldsymbol{a}(-j\omega) - \boldsymbol{b}^T(j\omega)\boldsymbol{b}(-j\omega) . \tag{111}$$

An additional mathematical manipulation leads to the final forging of a design strategy for lossless two port filters. In particular, observe from (32) that the incident and reflected variables of a two port network interrelate as the matrix relationship,

$$\boldsymbol{b}(j\omega) = \boldsymbol{S}(j\omega)\boldsymbol{a}(j\omega) , \tag{112}$$

for which

$$\boldsymbol{b}(-j\omega) = \boldsymbol{S}(-j\omega)\boldsymbol{a}(-j\omega) \tag{113}$$

and

$$\boldsymbol{b}^T(j\omega) = \left[\boldsymbol{S}(j\omega)\boldsymbol{a}(j\omega)\right]^T = \boldsymbol{a}^T(j\omega)\boldsymbol{S}^T(j\omega) . \tag{114}$$

Equation (111) now becomes, with the help of (113),

$$P_{avg} = \boldsymbol{a}^T(j\omega)\boldsymbol{a}(-j\omega) - \boldsymbol{a}^T(j\omega)\boldsymbol{S}^T(j\omega)\boldsymbol{S}(-j\omega)\boldsymbol{a}(-j\omega) ,$$

or

$$P_{avg} = \boldsymbol{a}^T(j\omega)\left[\boldsymbol{U} - \boldsymbol{S}^T(j\omega)\boldsymbol{S}(-j\omega)\right]\boldsymbol{a}(-j\omega) , \tag{115}$$

where $\boldsymbol{U}$ is the identity matrix. Although this relationship has been derived for the specific case of a two port linear network, it is applicable to the more generalized environment of an m–port multiport. For an m–port, $\boldsymbol{U}$ is an identity matrix of order $m$, and $\boldsymbol{S}$ is a square matrix, also of order $m$.

## 4.3. LOSSLESS, PASSIVE TWO PORT NETWORK

The lossless condition for a two port network is rendered transparent by (115); specifically,

$$\boldsymbol{U} \equiv \boldsymbol{S}^T(j\omega)\boldsymbol{S}(-j\omega). \tag{116}$$

Returning to the two port network case, (116) implies

$$\begin{bmatrix} 1 & 0 \\ 0 & 1 \end{bmatrix} = \begin{bmatrix} S_{11}(j\omega) & S_{21}(j\omega) \\ S_{12}(j\omega) & S_{22}(j\omega) \end{bmatrix} \begin{bmatrix} S_{11}(-j\omega) & S_{12}(-j\omega) \\ S_{21}(-j\omega) & S_{22}(-j\omega) \end{bmatrix}. \tag{117}$$

Equivalently,

$$\left|S_{11}(j\omega)\right|^2 + \left|S_{21}(j\omega)\right|^2 = 1, \tag{118}$$

$$\left|S_{22}(j\omega)\right|^2 + \left|S_{12}(j\omega)\right|^2 = 1, \tag{119}$$

$$S_{11}(j\omega)S_{12}(-j\omega) + S_{21}(j\omega)S_{22}(-j\omega) = 0, \tag{120}$$

and

$$S_{12}(j\omega)S_{11}(-j\omega) + S_{22}(j\omega)S_{21}(-j\omega) = 0. \tag{121}$$

Since the transducer power gain, $G_T(j\omega)$, which is intimately related to the reference-terminated voltage gain in accordance with (38), is the squared magnitude of S–parameter $S_{21}$, (118) implies

$$\left|S_{11}(j\omega)\right|^2 = S_{11}(j\omega)S_{11}(-j\omega) = 1 - G_T(j\omega). \tag{122}$$

As is demonstrated in a forthcoming example, this relationship is the foundation upon which rests the design strategy governing the realization of a lossless two port filter satisfying any realistic frequency response requirement. In particular, the transducer power gain can be computed via (38) for a given or desired input voltage -to- output voltage frequency response. For example, this frequency response may reflect a Butterworth, Chebyschev, Bessel, or any other meaningful lowpass, bandpass, highpass, notch, or other frequency response form. Then the squared magnitude of parameter $S_{11}$ can be factored into a product of a complex number and its conjugate, whence the input impedance under reference terminated output port conditions can be discerned. This input impedance function can then be expanded as a continued fraction expansion to arrive at the required filter topology. It is important to underscore the fact that since (122) applies to a lossless electrical complex, the elemental nature of the input impedance commensurate with the foregoing design procedure is either inductive or capacitive. Therefore, this impedance is necessarily proportional to a ratio of a numerator polynomial in $(j\omega)$ -to- a denominator polynomial in $(j\omega)$, the orders of which differ precisely by one.

## EXAMPLE #3:

A communication system application requires a lowpass, third order Butterworth filter that provides a *3-dB* bandwidth of $B = 2\pi(1.2\ GHz)$. The filter is to drive a *50* $\Omega$ resistive load $(R_l)$ from an antenna whose coupling to the filter is a coaxial cable having a characteristic impedance that is likewise *50* $\Omega$ $(R_s)$. Realize the filter as a lossless (LC) two port topology.

## SOLUTION:

**(1).** The conceptual schematic diagram of the required lossless filter is offered in Figure (15a). The terminating load resistance is $R_l = 50\ \Omega$ and the effective Thévenin source resistance is $R_s = 50\ \Omega \equiv R_l$. Since the filter is lossless and therefore contains only presumably ideal inductances and capacitances as branch elements, and since the requisite two port delivers a lowpass frequency response, the zero frequency voltage "gain" is simply the divider $R_l/(R_l + R_s)$, or $0.5$.

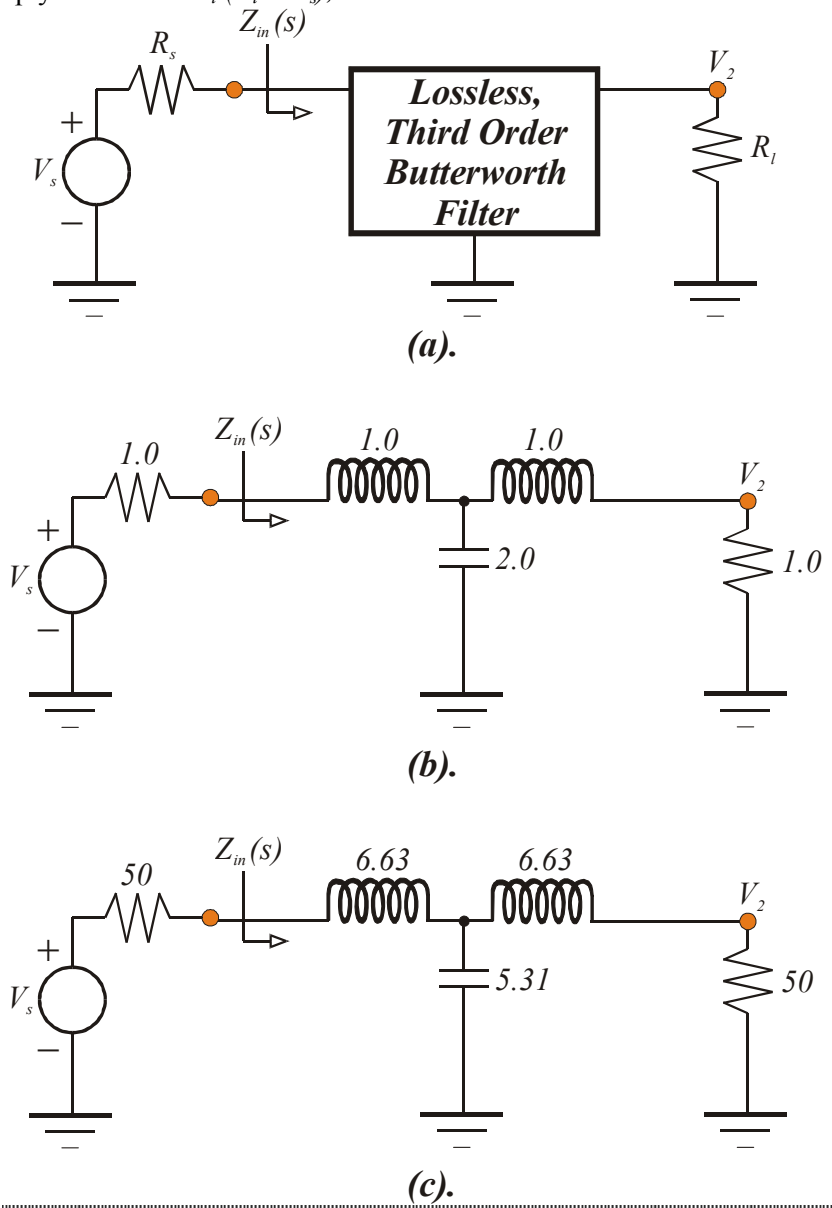


**Fig. (15).** **(a).** System Level Abstraction Of The Filter Design Problem Addressed In Example #3. **(b).** The Normalized Filter Realization. Resistances Are Referred To $50\ \Omega$, Inductances To $6.6315\ nH$, And Capacitances To $2.6526\ pF$. **(c).** Filter Realizing A Third Order Butterworth Response. All Resistances Are In Ohms, Inductances are In Nanohenries, And The Capacitance Is In Units of Picofarads. The $3\text{-}dB$ Frequency Of The Lowpass Filter Is $1.2\ GHz$.

**(2).** The third order Butterworth polynomial for a lowpass filter whose *3-dB* bandwidth is normalized to *1 Hz* is, in terms of the Laplace operator, *"s,"* $(s+1)(s^2+s+1)$, which means that the voltage transfer function of the system abstracted in Figure (15a) is

$$H(s) = \frac{V_2}{V_s} = \frac{0.5}{(1+s)(1+s+s^2)} .$$

From (38), this result implies a requisite transducer power gain, $G_T(s)$, of

$$G_T(s) = |S_{21}(s)|^2 = |2H(s)|^2 = 4H(s)H(-s) = \frac{1}{1-s^6} .$$

**(3).** Using (122), the scattering parameter, $S_{11}$, satisfies

$$|S_{11}(s)|^2 = 1 - G_T(s) = \frac{-s^6}{1-s^6} .$$

Since the squared magnitude of $S_{11}(s)$ is the product of $S_{11}(s)$ and its conjugate, $S_{11}(-s)$,

$$S_{11}(s) = \frac{s^3}{(1+s)(1+s+s^2)} ,$$

where the factoring of the denominator of the squared magnitude of $S_{11}(s)$ is facilitated by the observation that the poles of $S_{11}(s)$ are necessarily the same as the poles of the desired voltage transfer function.

**(4).** Recalling (35), the required input impedance function is

$$Z_{in}(s) = R_o\left[\frac{1+S_{11}(s)}{1-S_{11}(s)}\right] = R_o\left(\frac{1+2s+2s^2+2s^3}{1+2s+2s^2}\right),$$

with the understanding that the subject input impedance is that which materializes when the output port of the filter is terminated in the requisite load resistance, $R_l$. Ordinarily, the constant multiplier, $R_o$, in this impedance relationship is taken to be the source resistance, $R_s$. In this case, the source and load resistances are matched to ensure unity transducer power gain at low frequencies. Thus, $R_o$ in the present case is either $R_s$ or $R_l$, both of which happen to be *50 Ω*.

The frequency in all of the foregoing performance relationships has been normalized to the desired filter bandwidth of $B = 2\pi(1.2\ GHz)$; that is, *1.0 Hz* corresponds to *1.2 GHz*. If circuit branch impedances are normalized to $R_o$, *1.0 Ω* corresponds to *50 Ω*. The synthesis procedure is expedited, at least in a numerical sense, by proceeding to normalize all inductive and capacitive impedances at the circuit bandwidth to the reference, or normalizing, resistance $R_o$. Thus, if $L_\alpha$ symbolizes the normalizing inductance,

$$L_\alpha = \frac{R_o}{B} = 6.6315\ nH ,$$

meaning that *1.0 H* in the circuit realization maps to *6.6315 nH* in the finalized design. For branch capacitances,

$$C_\alpha = \frac{1}{BR_o} = 2.6526\ pF .$$

Thus, *1.0 F* in the realization is in one -to- one correspondence with an actual branch capacitance of *2.6526 pF*. It follows that the impedance to be synthesized derives from the normalized expression,

$$Z_{in}(s) = \frac{1 + 2s + 2s^2 + 2s^3}{1 + 2s + 2s^2}.$$

**(5).** A continued fraction expansion (essentially repeated long division) of the foregoing impedance function results in

$$Z_{in}(s) = s + \frac{s+1}{2s^2 + 2s + 1} = s + \frac{1}{2s + \frac{1}{s+1}}.$$

The far right hand side of this equation infers the normalized circuit offered in Figure (15b). In particular, the circuit is a *1.0 H* inductance connected in series with a topology consisting of a *2.0 F* capacitance shunting a series combination of a *1.0 H* inductance and a *1.0 Ω* resistance. The subject *1.0 Ω* resistance is, of course, the normalized load termination. Figure (15c) portrays the de-normalized, or actual, lossless filter required by the given operating specifications.

**COMMENTS:** The SPICE simulation of the magnitude response for the filter in Figure (15c) is shown in Figure (16). Note a response magnitude that is flat to within nominally three decibels up to a frequency of *1.2 GHz*, which is the *3-dB* bandwidth objective of the design.

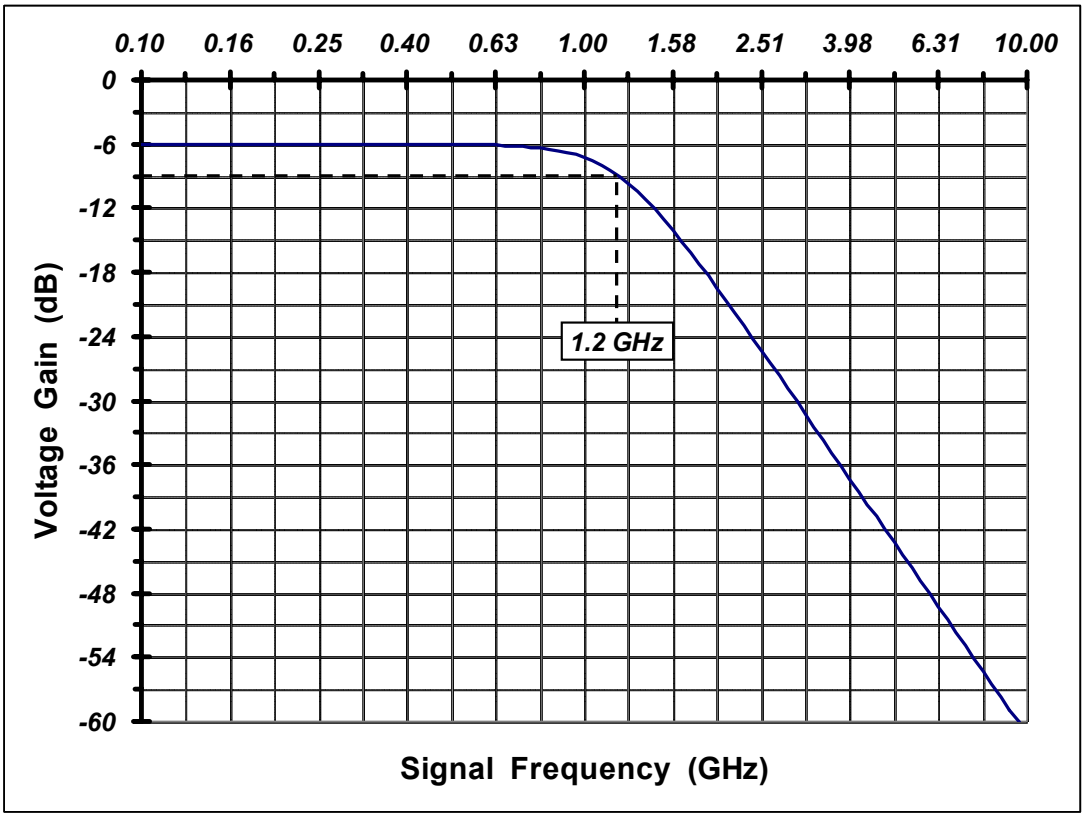


**Fig. (16).** SPICE Simulation Of The Frequency Response For The Third Order, Lowpass Butterworth Filter Given In Figure (15).

Although the filter design procedure exemplified herewith is most easily applied to the problem of realizing lowpass filter architectures, the resultant lowpass architecture can form the basis for other types of frequency response forms. In particular, well-known frequency response transformation tools can transform a prototype lowpass filter into a bandpass,

highpass, notch, or other type of filter[4]. For example, Figure (17) submits a bandpass filter architecture predicated on the lowpass structure designed in this example. In effect, observe that inductances appearing in the lowpass structure are supplanted by series-resonant LC circuits, while capacitances in the lowpass circuit are replaced by parallel-resonant LC branches. The indicated element values in Figure (17) pertain to a tuned center frequency of $2\pi(1.2\ GHz)$ and a *3-dB* bandwidth of *300 MHz*, which implies an effective quality factor of four. The SPICE frequency response plot in Figure (18) confirms the functionality of the bandpass structure.

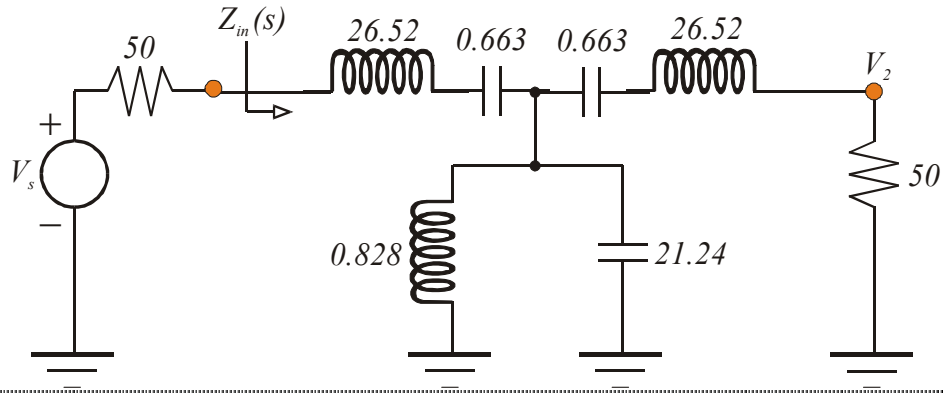


**Fig. (17).** Butterworth Bandpass Filter Realized By Applying A Lowpass -To- Bandpass Frequency Transformation To The Lowpass Filter In Figure (15c). The Center Frequency Of The Filter Is Designed To Be *1.2 GHz*, And The *3-dB* Bandwidth Is Approximately *300 MHz*, Which Implies An Effective Quality Factor Of $Q = 4$.

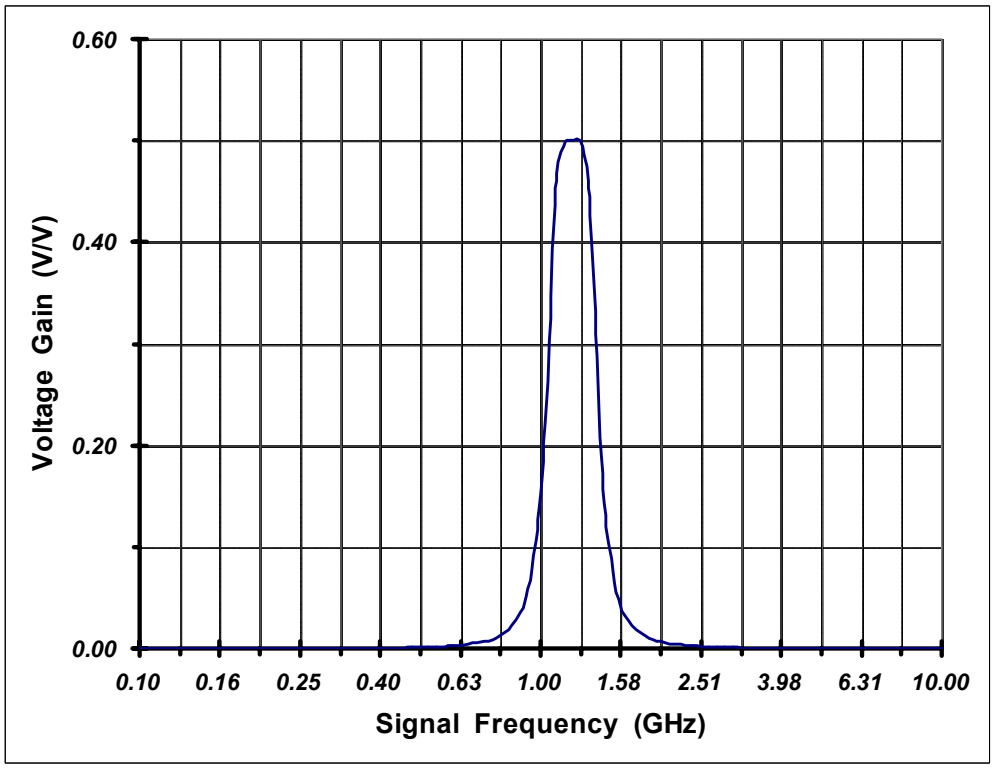


**Fig. (18).** SPICE Simulation Of The Frequency Response For The Third Order, Bandpass Butterworth Filter Given In Figure (17).

# 5.0. REFERENCES

[1]. P. H. Smith, "An Improved Transmission Line Calculator," *Electronics*, vol. 17, p. 130, Jan. 1944.

[2]. K. K. Clarke and D. T. Hess, *Communication Circuits: Analysis and Design*. Reading, Massachusetts: Addison-Wesley Publishing Company, 1978, pp. 444-447.

[3]. J. Choma, Jr., *Electrical Networks: Theory and Analysis*. New York: Wiley-Interscience, 1985, pp. 509-513.

[4]. W-K. Chen, *Passive and Active Filters: Theory and Implementations*. New York: John Wiley & Sons, 1986, pp. 92-101.